Sodium Late Current Blockers in Ischemia Reperfusion: Is the Bullet Magic?

Bruno Le Grand,[†] Christophe Pignier,[†] Robert Létienne,[†] Florence Cuisiat,[§] Françoise Rolland,[§] Agnes Mas,[§] and Bernard Vacher*[,§]

Pierre Fabre Research Center, 17 Avenue Jean Moulin, 81106 Castres Cedex, France

Received January 31, 2008

We describe the discovery of the first selective, potent, and voltage-dependent inhibitor of the late current mediated by the cardiac sodium channel $Na_V1.5$. The compound 3,4-dihydro-*N*-[(2*S*)-3-[(2-methoxyphenyl)thio]-2-methylpropyl]-2*H*-(3*R*)-1,5-benzoxathiepin-3-amine, **2a** (F 15845), was identified from a novel family of 3-amino-1,5-benzoxathiepine derivatives. The late sodium current inhibition and antiischemic effects of **2a** were studied in various models in vitro and in vivo. In a rabbit model of ischemia−reperfusion, **2a** exhibited more potent antiischemic effects than reference compounds KC 12291, ranolazine, and ivabradine. Thus, after a single administration, **2a** almost abolished ST segment elevation in response to a transient coronary occlusion. Further, the antiischemic activity of **2a** is maintained over a wide range of doses and is not associated with any hemodynamic changes, contrary to conventional antiischemic agents. The unique pharmacological profile of **2a** opens new and promising opportunities for the treatment of ischemic heart diseases.

Introduction

The activation of voltage-gated sodium channels in cardiac cells generates at least two types of inward currents (I_{Na}[a]), a transient (<3 ms), large amplitude one and another of weak intensity that spans the action potential (>300 ms).[1] The former initiates the rapid upstroke of the action potential (AP), whereas the other, referred as persistent (or late) sodium current, has no well-defined function although it participates in the duration of the AP.[2,3] Under normal physiological conditions, the late I_{Na} represents only a small fraction of the total Na^+ currents (<1%). However, when cells are subjected to long depolarization (e.g., myocardial ischemia), that late component is substantially amplified.[4]

During ischemia−reperfusion, the increased intracellular concentration of Na^+ is considered to be the driving force for the Ca^{2+} overload that contributes to cell damage and death.[5,6] Although there is much controversy surrounding the pathway(s) involved in sodium loading,[7] we contended that the late I_{Na} constitutes the main source of sodium in ischemic myocardium. Accordingly, preventing prolonged sodium entry through the Na^+ channel should improve Na^+ homeostasis, attenuate secondary intracellular Ca^{2+} accumulation, and therefore halt or slow the ischemic process.[8]

In the late 1970s it was reported that the late component of Na^+ currents was more sensitive to tetrodotoxin (TTX)[9] than its rapid counterpart,[10] demonstrating thus that independent modulation of each component is feasible.[11] This observation provides the rationale[12] for our intervention. Because voltage-gated sodium channels (Na_V) are ubiquitous, diverse, and highly dynamically regulated,[13] the ideal Na^+ blocker aimed at myocardial ischemia should (1) interact selectively with the $Na_V1.5$ isoform, which is the predominant pore-forming α-subunit in the heart, (2) spare any other channels (e.g., Ca^{2+}, K^+) and ionic transport systems (e.g., pumps, exchangers), and (3) depress the late component of Na^+ currents preferentially. Such features greatly differ from the attributes of Na^+ blockers in clinical use, which are neither isoform nor even channel selective (i.e., class I antiarrhythmics,[14] anticonvulsants, and local anesthetics).

The starting point of our medicinal chemistry program was the tripeptide IFM (isoleucine−phenylalanine−methionine). This cluster of amino acids is located in the III−IV inside loop of the Na^+ channel and plays an essential role in channel gating.[15] The nature of the channel modification(s) that results in dramatic enhancement of late I_{Na} during ischemia is unknown at the molecular level. We assume, however, that it originates from incomplete fast inactivation due to impede docking of the IFM motif at its binding site within the pore of the channel. Indeed, this approach extends from work of several groups on "neuronal" and "skeletal muscle" Na^+ channels where it has been demonstrated that (1) exogenous IFM-containing peptides can restore fast gating to channels that have switched into a slow-inactivating mode following various alterations (e.g., mutations, deletions)[16] and (2) fast-inactivated channels cannot enter the slow-inactivated state until the cell membrane has been repolarized (i.e., until the next cardiac cycle).

Conformational examination of IFM sequence revealed the possible existence of a stabilizing interaction between the sulfur of M (methionine) and the phenyl of F (phenylalanine) that may restrain the flexibility of the peptide (Figure 1).[17] This observation prompted us to search for nonpeptidic molecules that would mimic the folded conformation of the IFM predicted by calculations,[18] on the grounds that such products would benefit from phamacokinetic and entropic advantages (upon binding) over the tripeptide and the like. Thus, we began to explore benzothiacyclanes as a means of ensuring sulfur−phenyl proximity and better controlling the spatial arrangement of the substituents positioned in its periphery. After some vain attempts at late I_{Na} blockade, rewards finally came from 3-amino-1,5-benzoxathiepine derivatives carrying a chain that resembles that of ranolazine[19] (**1a**, Figure 2). Our next productive move was

* To whom correspondence should be addressed. Phone: (+33) 56371 4222. Fax: (+33) 56371 4299. E-mail: bernard.vacher@pierre-fabre.com.
[†] Cardiovascular 2 Division.
[§] Medicinal Chemistry 1 Division.

[a] Abbreviations: I_{Na}, inward sodium current; AP, action potential; TTX, tetrodotoxin; Na_V, voltage-gated sodium channel; IFM, isoleucine−phenylalanine−methionine; BOC, *tert*-butoxycarbonyl; VIDC, veratridine induced diastolic contracture; HEK, human embryonic kidney; HP, holding potential; LPH, Langendorff perfused heart.

10.1021/jm800100z CCC: $40.75
Published on Web 06/05/2008

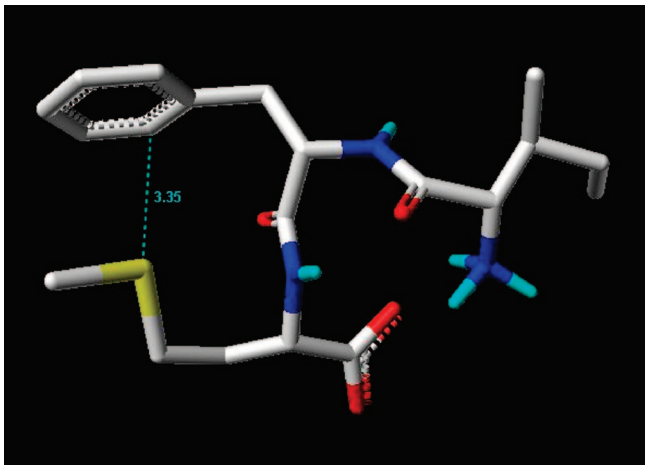

Figure 1. Low-energy conformer of IFM. The interaction between the sulfur of M and the phenyl group of F is indicated by a blue line. Hydrogen atoms are omitted.

to replace the oxygen in the catechol-like function of **1a** by a sulfur atom (see **1b**). Here, we focused on optimization of the substituent in position 2 on the chain (see tables for numbering), keeping the 1,5-benzoxathiepine core unchanged. This effort culminated in the selection of the clinical candidate **2a** (F 15845, Figure 3).[20] To illustrate the advantages of **2a** over the late I_{Na} blockers KC 12291[21] and ranolazine and over the recently marketed antiischemic drug ivabradine[22] (Figure 2), we compare and discuss the results obtained in a classical in vivo model of ischemia−reperfusion.

Chemistry

The synthetic routes used for the preparation of compounds **2a**−**d**, **16**, **17**, **19**−**21**, and **25**−**27** are described in Scheme 1. Alkylation of enantiomerically enriched oxazolidinone **3**[23] with trimethylorthoformate, according to Evans,[24] produced **4** diastereoselectively. The reduction of **4**[25,26] with lithium borohydride in the presence of water[27] provided the corresponding alcohol, which was then activated as a tosylate (**5**). Displacement of the tosyl group with 2-methoxyphenylthiolate and hydrolysis of the dimethylacetal function under mild acid conditions delivered the aldehyde **6** (R_1 = nPr) without racemization. Alternatively, commercially available or known enantiomerically enriched derivatives **7** or **8**[28] were converted to thioethers **9**[29] by treatment with 2-methoxythiophenol and then oxidized to aldehydes **6**[30] (R_1 = H, F, Me, Et, iPr) by a modified Swern reaction.[31] The sensitive aldehydes **6** were generally not isolated but engaged directly in the reductive amination step. Thus, reaction between **6** and 3-(*R*)- or 3-(*S*)-3-amino-1,5-benzoxathiepine[32] generated compounds **2a**−**d**, **16**, **17**, and **25**−**27**. On the other hand, the primary alcohol function in chiral 1,2-propanediols **10**[33] was first masked as a trityl ether (**11**)[34] and then the secondary alcohol function alkylated to give **12**. From **12**, cleavage of the protecting group produced **9** (R_1 = OMe, OEt, OPr), which was oxidized and converted into derivatives **19**−**21** as described above.

Scheme 2 summarizes the preparation of compounds **18**, **22**, and **23**. Thus, racemate or enantiomerically enriched 1-(2-methoxyphenylthio)-2,3-epoxypropane **13** reacted with 3-(*R*)- or 3-(*S*)-amino-1,5-benzoxathiepine to give **18**, regioselectively. Subsequent protection of **18a** as a BOC-carbamate (**14**) followed by acylation of the secondary hydroxyl function and removal of the N-protecting group afforded products **22** and **23**.

Access to the unsaturated derivatives **24** and **28** is depicted in Scheme 3. The thioether intermediates **15** were obtained from 2-methoxybenzenethiol and the known dichloroalkenes.[35] Condensation of **15** with 3-(*R*)-amino-1,5-benzoxathiepine then furnished products **24** and **28** in a straightforward manner.

Results and Discussion

For compound optimization we relied on in vitro models designed to mimic ischemia and to reproduce the late component of sodium currents. Two of the assays exploit the capacity of veratridine to block the sodium channels in a conducting state at resting membrane potential.[36] Thus, our primary screen uses the diastolic contracture of the rat isolated left atrium induced by veratridine (VIDC). This model has been extensively characterized[37] and, importantly, is known to be resistant to inhibition by conventional antiischemic agents.[38] For rapid selection of molecules, all compounds were evaluated at a single concentration (1 μM) and a 40% reduction of atrial contracture was set as lower limit for activity, on the basis of that observed with KC 12291 (see Table 2). Compounds above that threshold were further investigated in isolated Langendorff perfused beating hearts from guinea pigs, a model of global ischemia.[39] In the latter, we measure the capacity of the compounds to reduce the contracture that develops upon prolonged interruption of the coronary circulation. Thus, unlike the previous VIDC model, which depends on direct Na^+ channel activation, this one is ischemia-induced and therefore more closely simulates the clinical situation.

According to the mechanistic scenario we adhere to (see Introduction), the ischemic contracture is a remote, indirect consequence of inactivation failure of Na^+ channels. So we next examined the ability of the compounds to block late Na^+ current in a recombinant system expressing human $Na_V1.5$ channels.

The lead structure **1** (Figure 2) contains two stereogenic tertiary carbons: one at C3 on the oxathiepine ring and the other at C2 on the chain. To avoid dealing with mixture of stereoisomers during the optimization process, we cleared up the stereochemistry issue at the onset, assuming that the 3D SAR will be preserved throughout the study. Initially, the active configuration at C3 and C2 was deduced from the comparison between diastereoisomers **18ab** and **18cd** and epimers **18a** and **18b**, respectively (Table 1). As shown in Table 1, the enantiomerically "pure" derivatives **18a** and **2a** are the most efficacious against both VIDC and the late I_{Na} (vs **18b** and **2b**−**d**, respectively). In the course of the project we confirmed on several occasions that late I_{Na} blockade was associated with this specific stereochemical pattern.[40] In retrospect, the coherence of the 3D SAR suggests that derivatives of this series act at a unique, geometrically well-defined site on the $Na_V1.5$ protein.

With the absolute configuration required for optimum activities secured, SAR was explored by varying the nature of the groups at C2 (Table 2).

Among the compounds listed in Table 2, several reduce atrial contracture with a magnitude exceeding 40% (i.e., **2a**, **18a**, **19**, **20**, **25**, **27**, and **28**). Of these, four exhibit an activity in the range of that of KC 12291 (i.e., **18a**, **19**, **20**, and **28**) whereas three (**2a**, **25**, and **27**) have an activity that even surpassed that of TTX. It is clear that a substituent at C2 is required for antiischemic efficacy (see **16**).[41] When we tried to delineate the role of the C2-OH in **18a**, we noticed that this group did not interchange with fluorine[42] (**17**) and that a methyl ether was just as active (**19** vs **18a**), questioning the contribution of any H-bond interaction in its activity. In the C2-ether subset, a two-carbon chain seems the maximum length accommodated (**19**, **20** vs **21**).

On the other hand, an ester function at C2 ruins the VIDC activity (cf. **22** and **23**), whereas an aliphatic substituent at this

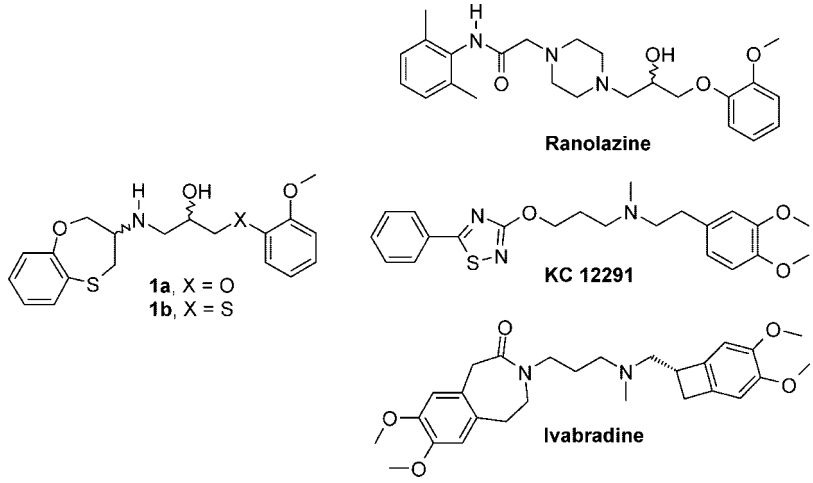

Figure 2. Structures of the lead compound **1**, ranolazine, KC 12291, and ivabradine.

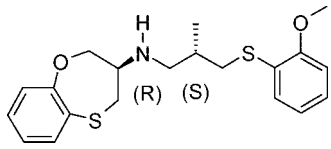

Figure 3. Structure of compound **2a** (F 15845).

position improves it markedly (cf. **2a**). In fact, the larger the alkyl group, the greater is the inhibition achieved in the VIDC; again, two contiguous carbons seem to be the limit tolerated (**25** and **27** > **26**). The stereochemical "pressure" exerted at C2 resurfaces through the outcomes of **24** and **28** where a planar arrangement (i.e., sp^2-C2) compromises the antiischemic activity (**24** vs **2a**).[41]

Overall, these results support the existence of a favorable hydrophobic interaction between the group at C2 and the substrate−protein, this interaction being subjected, however, to strict restrictions in terms of size and orientation (see **26**).

In Lagendorff perfused hearts, the number of compounds affording protection against ischemia-induced contracture narrowed down sharply, emphasizing the greater discriminating power of that model (referred hereafter as LPH) compared to the VIDC one. The derivatives that passed are, however, all more active than KC 12291 (i.e., **2a**, **19**, and **25**), even though the inhibition showed by **19** has to be tempered by the modest activity it attains in the VIDC paradigm. In contrast, compounds **2a** and **25** give fairly comparable responses in both models. Further, under baseline conditions, they have no significant impact on hemodynamic variables (data not shown).

At this juncture, the antiischemic activity observed in VIDC and LPH needed to be related somehow to blockade of the late I_{Na} current. To this end, the influence of the compounds on sodium conductance was probed in HEK cells transfected with the $hNa_V1.5$ isoform. Compound **19** hardly interferes with the late I_{Na} component despite its ability to counteract ischemic contracture both in isolated atria and in intact hearts, implying that element(s) other than I_{Na} blockade are at play in its antiischemic action. In contrast, compounds **2a** and **25** effectively and reversibly decrease late I_{Na}. For instance, at 10 μM, compound **2a** diminishes current amplitude by 70 ± 5% from a holding potential of −90 mV, approaching that obtained with TTX and greater than that of KC 12291. Compound **18a** has a profile similar to that of KC 12291; it is active against late I_{Na} and VIDC but not against LPH. Although, late I_{Na} blockade and VIDC reduction roughly follow the same trend, which is not unexpected since they share the same causal mechanism (Na^+ channels overactivation), there is no obvious correlation between late I_{Na} and LPH.[43] Collectivelly, inhibition of late I_{Na} appears to be sufficient for providing antiischemic activity (e.g., **2a** and **25** vs **19**) but it is not mandatory.

In addition, with **2a**, inhibition of the late I_{Na} is more pronounced at −90 mV than at −110 mV (IC_{50} = 2.56 ± 0.54 μM vs 5.77 ± 2.01 μM, Figure 4). This shift of the inactivation in the depolarized direction indicates that blockade of the channels is more effective under conditions in which prolonged depolarizations are likely to occur (see Introduction). This may have profound therapeutic relevance in that inhibition of the sodium current by **2a** should increase as pathological activation of the channel grows. In other words, **2a** is potentially "ischemia-selective". At a molecular level, the voltage-dependence may just reflect the accessibility of the site of interaction of these molecules on the $Na_V1.5$ protein. With **2a**, this site is available only within a limited range of membrane potential. In comparison, **25** is less (if not) voltage-sensitive than **2a** and KC 12291 is equally active at both −90 and −110 mV.

Finally, only two derivatives **2a** and **25** match all the criteria defined at the outset: they produce high antiischemic effects in two different in vitro models and do so by blocking late I_{Na} selectively.[44] To further evaluate the potential of **2a**, it was studied with references in a preclinical rabbit model of myocardial ischemia. The latter uses the increase in ST segment amplitude following coronary occlusion as a highly sensitive and robust marker of myocardial ischemia.[45]

After single, bolus iv administration, compound **2a** dose-dependently reverses ischemia-induced ST segment elevation with an ED_{50} value of 0.05 mg/kg (Figure 5A).[46] From 0.08 mg/kg to the largest dose tested (2.5 mg/kg) the compound almost normalizes electrical activity during coronary occlusion−reperfusion. The span of "active" doses is indeed remarkable; moreover, throughout the whole range of doses (0.01−2.5 mg/kg), **2a** was devoid of effect on arterial pressure or heart rate.[47] Among the references, only ivabradine produces dose-dependent inhibition of ST segment elevation. It is, however, more than 10-fold less potent (ED_{50} = 0.59 mg/kg) than **2a**. Although ivabradine also nearly abolishes ST changes at 2.5 mg/kg (Figure 5C), it exerts a pronounced, dose-related bradycardia from 0.16 mg/kg upward.[47] This illustrates a major difference between the mechanisms of action of these two products, and in our view, this also constitutes a serious limitation to the usefulness of

Scheme 1. Synthesis of Compounds **2**, **16**, **17**, **19**−**21**, and **25**−**27**[a]

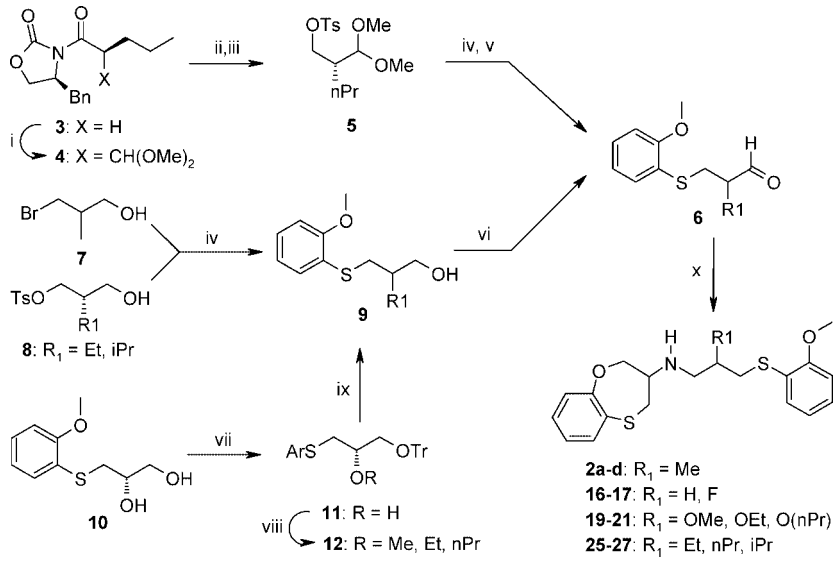

[a] Reagents and conditions: (i) $CH(OMe)_3$, $TiCl_4$, $EtNiPr_2$; (ii) $LiBH_4$, THF; (iii) TsCl, Py, DMAP; (iv) ArSH, base; (v) $ArSO_3H$, Me_2CO, H_2O; (vi) $(COCl)_2$, DMSO, NEt_3, CH_2Cl_2; (vii) trityl-Cl, C_5H_5N, CH_3CN; (viii) NaH, RX, THF; (ix) HCl, EtOH; (x) (*R*)- or (*S*)-3-3-amino-1,5-benzoxathiepine, $NaBH(OAc)_3$, $C_2H_4Cl_2$.

Scheme 2. Synthesis of Compounds **18**, **22**, and **23**[a]

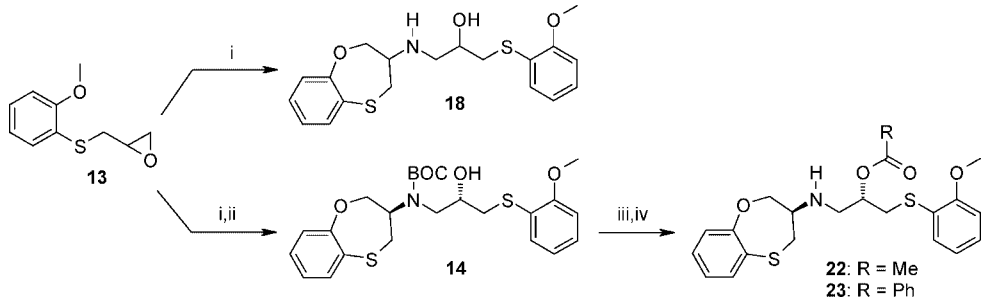

[a] Reagents and conditions: (i) (*R*)- or (*S*)-3-amino-1,5-benzoxathiepine, Na_2CO_3, iPrOH, reflux; (ii) $(BOC)_2O$; (iii) RCOCl, NEt_3, CH_2Cl_2; (iv) TFA, CH_2Cl_2.

Scheme 3. Synthesis of Compounds **24** and **28**[a]

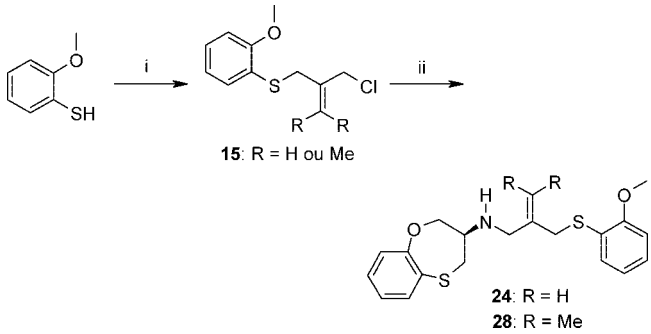

[a] Reagents and conditions: (i) dichloroalkene, K_2CO_3, acetone; (ii) (*R*)-3-amino-1,5-benzoxathiepine, Na_2CO_3, 100 °C.

ivabradine in certain categories of patients. The late I_{Na} blocker KC 12291 achieves only moderate reduction of ST segment elevation at 0.16 mg/kg, consistent with its in vitro profile (Table 2). Further, this inhibition is not dose-dependent, suggesting that beyond 0.16 mg/kg other factors that do not convey antiischemic activity manifest themselves (Figure 5B). Ranolazine (Figure 5D) affords some degree of protection but only at the higher dose tested (ED_{50} > 2.5 mg/kg), which again fits with its rather modest blockade of late I_{Na} (Table 2). At 2.5 mg/kg, the activity of ranolazin was not accompanied by hemodynamic changes.

Thus, compound **2a** elicits superior antiischemic properties in vivo relative to the recently marketed drugs ivabradine and ranolazine and relative to the I_{Na} blocker KC 12291. Importantly, the antiischemic activity of **2a** is free from any hemodynamic manifestation. The separation of antiischemic from hemodynamic properties indicates that **2a** acts directly on the cardiomyocite, which clearly distinguishes it from most known antiischemic agents.

Conclusions

In this work, we describe the process through which we discovered a structurally novel family of cardiac sodium channel blockers. Several compounds of this family interact selectively with the $Na_V1.5$ isoform of the channel and preferentially block the late component of the currents. Subtle alterations in the structure or stereochemistry of the compounds dramatically affect their biophysic and antiischemic characteristics.

Among the derivatives prepared, **2a** blocks late I_{Na} very effectively and achieves high antiischemic effects in vitro and in vivo. Thus, in a rabbit model of regional ischemia, **2a** proves more potent and remains efficacious on a much broader range of doses than the antiischemic drugs ivabradine and ranolazine and the late sodium channel blocker KC 12291. In any case,

Table 1. 3D SAR, the Optimal Stereochemistry at C2 and C3

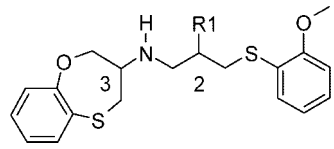

		absolute configuration			hNa$_v$1.5 channel blockade,[a] % inhib at 10 μM[c]	
compd	R_1	C2	C3	diastolic contracture, rat atrium (VI),[b] % inhib (1 μM)[c]	HP, −110 mV[d]	HP, −90 mV[e]
18ab	OH	*RS*	*R*	50 ± 7	37 ± 7	42 ± 4
18cd	OH	*RS*	*S*	26 ± 9	16 ± 5	21 ± 7
18a	OH	*S*	*R*	54 ± 5	69 ± 1	75 ± 11
18b	OH	*R*	*R*	7 ± 3	26 ± 6	30 ± 6
2a	Me	*S*	*R*	74 ± 3	53 ± 7	70 ± 5
2b	Me	*R*	*R*	38 ± 10	22 ± 6	34 ± 2
2c	Me	*S*	*S*	25 ± 9	31 ± 15	41 ± 11
2d	Me	*R*	*S*	26 ± 6	30 ± 2	44 ± 5

[a] Veratridine (40 μM) induced late sodium current in HEK cells expressing human Na$_v$1.5 channels. [b] Veratridine (40 μM) induced (VI) diastolic contracture in rat isolated left atrium. [c] Compound concentration used in the experiment. [d] Percentage of inhibition of late sodium current elicited at −30 mV from a holding potential of −110 mV. [e] Percentage of inhibition of late sodium current elicited at −30 mV from a holding potential of −90 mV.

Table 2. In Vitro SAR, optimization of R_1

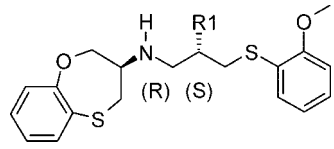

		diastolic contracture % inhib (1 μM)[e]		hNa$_v$1.5 channel blockade[a] % inhib. at 10 μM[e]	
compd	R_1	rat atrium (VI)[b,c]	GP intact heart[d]	HP −110 mV[f]	HP −90 mV[g]
16	H	3 ± 3			
17	F	32 ± 9	ND[h]	11 ± 3	19 ± 5
18a	OH	54 ± 5	14 ± 8	69 ± 1	75 ± 11
19	OMe	45 ± 5	64 ± 15	12 ± 3	27 ± 3
20	OEt	46 ± 4	33 ± 13	22 ± 16	34 ± 25
21	O(n-Pr)	30 ± 5	ND[h]	27 ± 13	27 ± 5
22	OCOMe	9 ± 11			
23	OCOPh	3 ± 19			
2a	Me	74 ± 3	65 ± 11	53 ± 7	70 ± 5
24	=CH_2	26 ± 12	ND[h]	36 ± 18	37 ± 17
25	Et	86 ± 6	68 ± 14	46 ± 5	54 ± 6
26	n-Pr	23 ± 9	ND[h]	17 ± 4	23 ± 6.
27	i-Pr	90 ± 1	31 ± 8	31 ± 9	34 ± 9
28	=CMe_2	42 ± 13	16 ± 11	31 ± 9	37 ± 6
KC 12291		45 ± 4	39 ± 22	60 ± 5	60 ± 5
ranolazine				11 ± 7	19 ± 7
TTX		64 ± 10	ND[h]	79 ± 2	87 ± 3

[a] Veratridine (40 μM) induced late sodium current in HEK cells expressing human Na$_v$1.5-channels. [b] Veratridine (40 μM) induced (VI) diastolic contracture in rat isolated left atrium. [c] A contracture of 40% was used as cutoff value. [d] 50 min of global ischemia induced contracture in isolated Langendorff perfused guinea pig (GP) heart. [e] Compound concentration used in the experiment. [f] Percentage of inhibition of late sodium current elicited at −30 mV from a holding potential (HP) of −110 mV. [g] Percentage of inhibition of late sodium current elicited at −30 mV from a holding potential of −90 mV. [h] ND: not determined.

the pharmacological profile of **2a** differs markedly from those of established antiischemic agents and conventional Na^+ blockers (i.e., class I antiarrhythmics, anticonvulsants, and local anesthetics).

Compound **2a** is heart-selective inasmuch as the channel isoform it targets (Na$_V$1.5) is prominently distributed in the myocardium. It is also ischemia-selective inasmuch as it can differentiate between the physiological and pathological activation of the channel (rapid vs late I_{Na}). From this combination, we anticipate that its therapeutic effectiveness will grow with the severity of the conditions and that side effects (motor and CNS) will be concomitantly limited.

As the first selective blocker of late Na$_V$1.5, compound **2a** should advance our understanding of the role of the late I_{Na} in myocardial ischemia. Hopefully, it will also open novel avenues in the treatment of heart diseases (e.g., recurrent angina, myocardial infarction, heart failure, arrhythmias, etc.) for which medical needs are still considerable.[48]

Experimental Section

Chemistry. Melting points were determined on a Büchi 530 melting point apparatus and were not corrected. ^{1}H NMR spectra were recorded on a Bruker Avance 400 spectrometer operating at 400 MHz for ^{1}H and 100 MHz for ^{13}C. Chemical shifts are reported in δ value (ppm) relative to an internal standard of tetramethylsilane. Infrared (IR) spectra were obtained on a Nicolet FT 510 P spectra photometer. Microanalyses were obtained on a Fison EA 1108/CHN analyzer. Mass spectra (TSQ 7000 Finnigan, Thermoelectron Corporation) were determined by electron spray ionization (ESI). Only 100% relative intensity peaks are given. Analytical thin-layer chromatography was carried out on precoated plates (silica gel, 60 F 254 Merck). The abbreviation "dr" refers to the percentage of one enantiomer over the mixture of stereoisomers; "er" refers to the percentage of one enantiomer over the racemate.

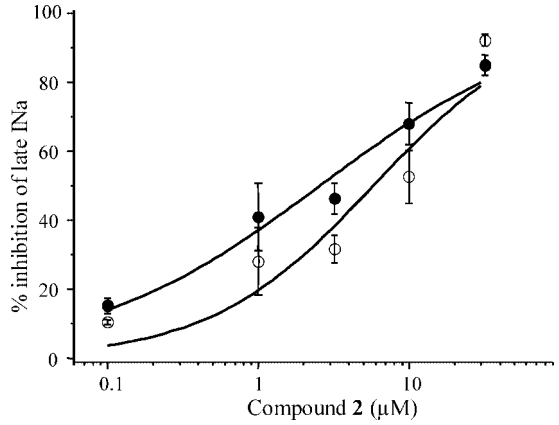

Figure 4. Effects of **2a** on persistent sodium current elicited at −30 mV from a holding potential of −110 mV (empty circles) and −90 mV (full circles).

General Method for the Reductive Amination between Aldehydes 6 and 3-Amino-1,5-benzoxathiepine. A solution of 3-amino-1,5-benzoxathiepine (1 equiv) in dry dichloromethane (10 mL/g) was added to the crude solution of the aldehyde **6** cooled at −20 °C. The reaction mixture was stirred for 20 min and then treated with sodium triacetoxyborohydride (1.2 equiv). Stirring was continued for 2 h at −10 °C. The reaction mixture poured into 10% aqueous sodium hydrogen carbonate solution and extracted with dichloromethane. The combined organic layer was washed with water and brine, dried over Na_2SO_4, filtered, and concentrated in vacuo. The free base was purified by flash column chromatography.

3,4-Dihydro-*N*-[(2*S*)-3-[(2-methoxyphenyl)thio]-2-methylpropyl]-2*H*-(3*R*)-1,5-benzoxathiepin-3-amine (2a). Crystallization of **2a** as a bromhydrate salt gave a white powder: mp = 139 °C; IR (KBr) 3377, 2659, 2591 ν cm^{-1}; ^1H NMR (CD_3OD) δ 1.20 (d, J = 8 Hz, 3H), 2.15−2.30 (m, 1H), 2.95−3.02 (dd, J = 13.4, 7.6 Hz, 1H), 3.02−3.08 (dd, J = 13.4, 8 Hz, 1H), 3.09−3.15 (dd, J = 12.7, 7.4 Hz, 1H), 3.16−3.26 (dd, J = 15.2, 3.2 Hz, 1H), 3.32−3.38 (ddd, J = 15.2, 5.9, 1.3 Hz, 1H), 3.42−3.47 (dd, J = 12.7, 6.4 Hz, 1H), 3.85 (s, 3H), 3.92 (m, 1H), 4.15 (d, J = 13.8 Hz, 1H), 4.64 (dd, J = 13.8, 2.9 Hz), 6.92−6.98 (m, 2H), 7.05−7.14 (m, 2H), 7.22−7.29 (m, 2H), 7.39−7.42 (dd, J = 7.6, 1.6 Hz, 1H), 7.44−7.46 (dd, J = 7.6, 1.6 Hz, 1H); ^{13}C NMR (CD_3OD) δ 18.3, 32.1, 33.0, 38.4, 51.8, 56.4, 59.5, 71.7, 112.4, 122.3, 123.4, 124.2, 125.8, 128.4, 129.5, 130.6, 132.4, 133.4, 159.6, 161.7; $[\alpha]_D^{25}$ −9.6° (*c* 0.18, CH_3OH); HPLC Chiralcel OD (Daicel) eluting with hexane/isopropanol, 80:20 (1 mL/min, UV, 220 nm), t_R = 13.8 min, 99.8% dr; MS (ESI) m/z = 376 [MH^+]. Anal. ($C_{20}H_{25}NS_2O_2 \cdot HBr$) C, H, N.

3,4-Dihydro-*N*-[(2*R*)-3-[(2-methoxyphenyl)thio]-2-methylpropyl]-2*H*-(3*R*)-1,5-benzoxathiepin-3-amine (2b). Crystallization of **2b** as a maleate salt gave a white powder: mp = 140 °C; IR (KBr) ν 3400, 2964, 1576, 1475 cm^{-1}; ^1H NMR (DMSO-d_6) δ 1.12 (d, J = 6.4 Hz, 3H), 2.13−2.51 (m, 1H), 2.83 (dd, J = 13.2, 7.2 Hz, 1H), 2.99−3.11 (m, 2H), 3.21 (dd, J = 12.0, 5.2 Hz, 1H), 3.29 (d, J = 4.4 Hz, 2H), 3.82 (s, 3H), 3.85 (m, 1H), 4.37 (d, J = 13.2 Hz, 1H), 4.47 (d, J = 13.2 Hz, 1H), 6.06 (s, 2H), 6.94−7.00 (m, 2H), 7.04−7.09 (m, 2H), 7.18−7.30 (m, 3H), 7.40 (d, J = 7.5 Hz, 1H); ^{13}C NMR (DMSO-d_6) δ 17.3, 30.3, 31.0, 35.0, 49.9, 55.6, 57.6, 70.4, 110.8, 121.0, 121.9, 124.1, 126.2, 126.6, 127.6, 127.7, 128.7, 131.4, 135.6 (2C), 156.3, 159.0, 167.2 (2C); $[\alpha]_D^{25}$ +52.4° (*c* 0.25, CH_3OH); HPLC Chiralcel OD (Daicel) eluting with hexane/isopropanol, 80:20 (1 mL/min, UV, 220 nm), t_R = 9.5 min, 97.3% dr. Anal. ($C_{20}H_{25}NS_2O_2 \cdot C_4H_4O_4$) C, H, N.

3,4-Dihydro-*N*-[(2*S*)-3-[(2-methoxyphenyl)thio]-2-methylpropyl]-2*H*-(3*S*)-1,5-benzoxathiepin-3-amine (2c). Crystallization of **2c** as a fumarate salt gave a white powder: mp = 131−133 °C; IR (KBr) ν 2969, 1656, 1575, 1476 cm^{-1}; ^1H NMR (DMSO-d_6) δ 1.00 (d, J = 6.4 Hz, 3H), 1.75−1.80 (m, 1H), 2.62 (d, J = 6.4 Hz, 2H), 2.69 (dd, J = 12.4, 8.0 Hz, 1H), 2.85 (dd, J = 13.6, 7.2 Hz, 1H), 3.03−3.13 (m, 2H), 3.81 (s, 3H), 3.85 (m, 1H), 3.94 (dd, J = 12.0, 6.0 Hz, 1H), 4.16 (dd, J = 12.4, 3.2 Hz, 1H), 6.61 (s, 2H), 6.91−7.00 (m, 4H), 7.13−7.20 (m, 2H), 7.26 (m, 1H), 7.34 (m, 1H); ^{13}C NMR (DMSO-d_6) δ 17.73, 33.2, 34.8, 35.4, 51.3, 55.6, 57.8, 74.3, 110.7, 120.9, 121.8, 123.5, 125.1, 126.1, 127.2, 127.6, 128.3, 131.4, 134.1 (2C), 156.2, 159.7, 166.1 (2C); $[\alpha]_D^{25}$ −45.6° (*c* 0.26, CH_3OH); HPLC Chiralcel OD (Daicel) eluting with hexane/isopropanol, 80:20 (1 mL/min, UV, 220 nm), t_R = 14.7 min, 96.5% dr. Anal. ($C_{20}H_{25}NS_2O_2 \cdot C_4H_4O_4$) C, H, N.

3,4-Dihydro-*N*-[(2*R*)-3-[(2-methoxyphenyl)thio]-2-methylpropyl]-2*H*-(3*S*)-1,5-benzoxathiepin-3-amine (2d). Crystallization of **2d** as a fumarate salt gave a white powder: mp = 131−133 °C; IR (KBr) ν 2966, 1709, 1655, 1573, 1474 cm^{-1}; ^1H NMR (DMSO-d_6) δ 1.08 (d, J = 6.8 Hz, 3H), 1.84−1.92 (m, 1H), 2.51−2.73 (m, 2H), 2.79 (dd, J = 12.0, 6.8 Hz, 1H), 2.96 (dd, J = 14.4, 7.2 Hz, 1H), 3.07−3.16 (m, 2H), 3.29 (m, 1H), 3.81 (s, 3H), 4.08 (dd, J = 12.4, 5.2 Hz, 1H), 4.24 (dd, J = 12.4, 2.8 Hz, 1H), 6.61 (s, 2H), 6.91−7.02 (m, 4H), 7.13−7.21 (m, 2H), 7.27 (d, J = 7.6 Hz, 1H), 7.35 (d, J = 7.6 Hz, 1H); ^{13}C NMR (DMSO-d_6) δ 17.6, 32.5, 33.9, 35.3, 50.8, 55.5, 57.6, 73.3, 110.6, 120.8, 121.8, 123.5, 124.8, 126.2, 127.2, 127.3, 128.3, 131.4, 134.3 (2C), 156.1, 159.5, 166.5 (2C); $[\alpha]_D^{25}$ 0° (*c* 0.30, CH_3OH); HPLC Chiralcel OD (Daicel) eluting with hexane/isopropanol, 80:20 (1 mL/min, UV, 220 nm), t_R = 10.9 min, 94.9% dr. Anal. ($C_{20}H_{25}NS_2O_2 \cdot C_4H_4O_4$) C, H, N.

3,4-Dihydro-*N*-[3-[(2-methoxyphenyl)thio]-propyl]-2*H*-(3*R*)-1,5-benzoxathiepin-3-amine (16). Compound **16** is purified by flash column chromatography (silica gel, dichloromethane/methanol, 92:8). Crystallization of **16** as a maleate salt gave a white powder: mp = 158−160 °C; IR (KBr) ν 3431, 1617, 1577, 1473 cm^{-1}; ^1H NMR (DMSO-d_6) δ 1.94−2.01 (m, 2H), 2.99 (t, J = 7.2 Hz, 2H), 3.20 (t, J = 7.2 Hz, 2H), 3.27 (m, 2H), 3.82 (s, 3H), 3.88 (s, 1H), 4.23 (d, J = 13.6 Hz, 1H), 4.46 (d, J = 12.4 Hz, 1H), 6.02 (s, 2H), 6.95−7.00 (m, 2H), 7.02−7.11 (m, 2H), 7.19−7.30 (m, 3H), 7.43 (dd, J = 7.6, 1.4 Hz, 1H); ^{13}C NMR (DMSO-d_6) δ 25.1, 27.4, 31.2, 43.9, 55.7, 56.9, 70.3, 110.9, 121.0, 122.1, 123.6, 124.3, 126.6, 126.8, 127.8, 129.0, 131.7, 135.8 (2C), 156.5, 159.4, 167.2 (2C); $[\alpha]_D^{25}$ +36.8° (*c* 0.47, CH_3OH); HPLC Chiralcel OD-H (Daicel) eluting with heptane/ethanol/diethylamine, 91:10:0.1 (1 mL/min, UV, 220 nm), t_R = 19.3 min, 99.1% er; MS (ESI) m/z = 362 [MH^+]. Anal. ($C_{19}H_{23}NO_2S_2 \cdot C_4H_4O_4$) C, H, N.

3,4-Dihydro-*N*-[(2*S*)-3-[(2-methoxyphenyl)thio]-2-fluoropropyl]-2*H*-(3*R*)-1,5-benzoxathiepin-3-amine (17). Compound **17** is purified by flash column chromatography (silica gel, dichloromethane/ethylacetate, 80:20). Crystallization of **17** as a maleate salt gave a white powder: mp = 151 °C; IR (KBr) ν 3447, 3006, 1577, 1473 cm^{-1}; ^1H NMR (DMSO-d_6) δ 3.17−3.51 (m, 6H), 3.79 (s, 1H), 3.84 (s, 3H), 4.27 (d, J = 13.2 Hz, 1H), 4.42 (d, J = 12.6 Hz, 1H), 4.99 (d, J = 48.3 Hz, 1H), 6.09 (s, 2H), 6.96 (t, J = 7.4 Hz, 1H), 7.04−7.09 (m, 3H), 7.25 (t, J = 7.5 Hz, 2H), 7.36 (d, J = 7.6 Hz, 1H), 7.41 (d, J = 7.5 Hz, 1H); ^{13}C NMR (DMSO-d_6) δ 31.4, 32.7 (d, J = 21.2 Hz), 47.3 (d, J = 20.9 Hz), 55.7, 57.2, 71.2, 89.5 (d, J = 173.1 Hz), 111.1, 120.9, 121.9, 122.7, 124.1, 126.6, 127.5, 128.8 (2C), 133.6, 134.8 (2C), 156.7, 159.4, 167.0 (2C); $[\alpha]_D^{25}$ +18.2° (*c* 0.43, CH_3OH); HPLC Chiralpak AD (Daicel) eluting with methanol (1 mL/min, UV, 220 nm), t_R = 12.8 min, 97.2% dr; MS (ESI) m/z = 380 [MH^+]. Anal. ($C_{19}H_{22}FNO_2S_2 \cdot C_4H_4O_4$) C, H, N.

3,4-Dihydro-*N*-[(2*S*)-3-[(2-methoxyphenyl)thio]-2-methoxypropyl]-2*H*-(3*R*)-1,5-benzoxathiepin-3-amine (19). Compound **19** is purified by flash column chromatography (silica gel, dichloromethane/ethylacetate, 90:10). Crystallization of **19** as a maleate salt gave a white powder: mp = 122 °C; IR (KBr) ν 3450, 2997, 1704, 1575, 1534 cm^{-1}; ^1H NMR (DMSO-d_6) δ 3.11−3.36 (m, 10H), 3.79 (s, 1H), 3.84 (s, 3H), 4.32 (d, J = 13.3 Hz, 1H), 4.49 (d, J = 12.4 Hz, 1H), 6.06 (s, 2H), 6.95−7.09 (m, 4H), 7.21−7.27 (m, 2H), 7.36 (d, J = 7.5 Hz, 1H), 7.40 (d, J = 7.4 Hz, 1H); ^{13}C NMR (DMSO-d_6) δ 31.1, 31.6, 47.1, 55.6, 56.5, 57.0, 70.5, 75.3, 110.9, 120.9, 121.9, 123.3, 124.1, 126.3, 127.2, 128.5, 128.8, 131.5, 135.4 (2C), 156.7, 159.2, 167.1 (2C); $[\alpha]_D^{25}$ −15.3° (*c* 0.30, CH_3OH); HPLC Chiralcel OD (Daicel) eluting with hexane/

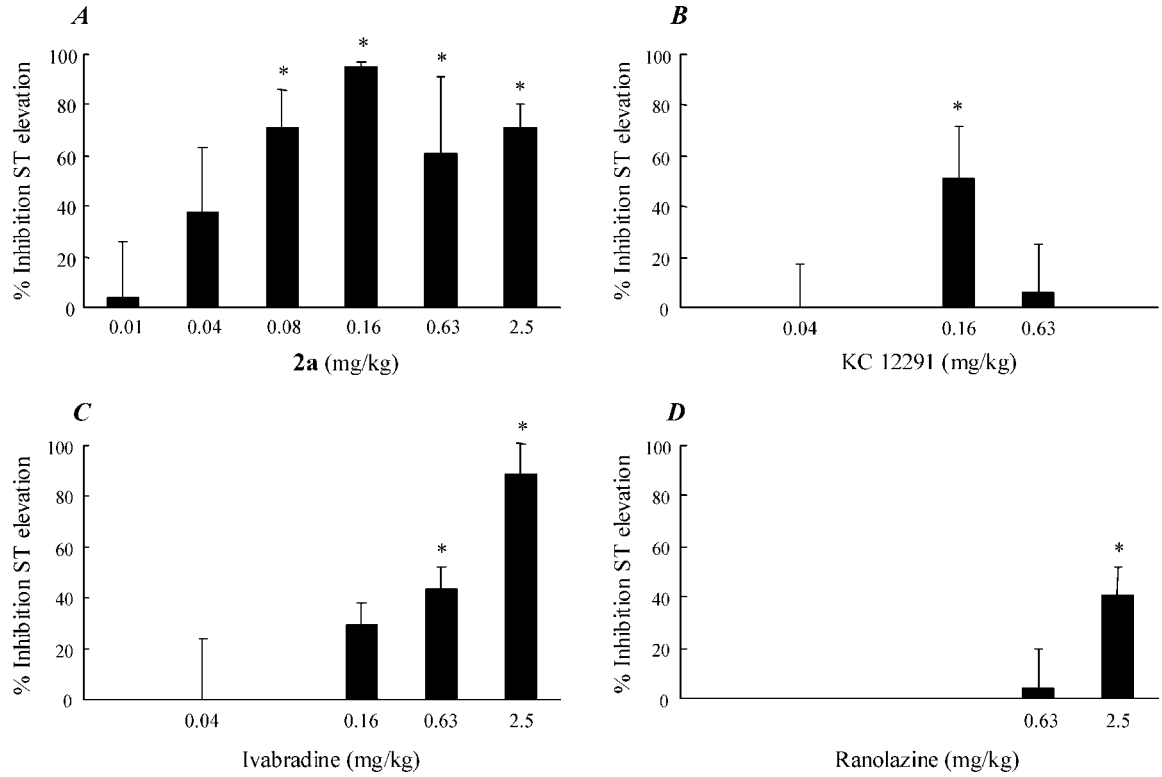

Figure 5. Dose-dependent inhibition of ST segment elevation by **2a** (A), KC 12291 (B), ivabradine (C), and ranolazine (D), administered iv 5 min before the coronary artery occlusion to pentobarbital-anesthetized rabbits. Data are mean values ± SEM: (*) $P < 0.05$ versus vehicle.

isopropanol, 90:10 (1 mL/min, UV, 220 nm), $t_R = 25.4$ min, 94.0% dr; MS (ESI) $m/z = 392$ [MH^+]. Anal. ($C_{20}H_{25}NO_3S_2 \cdot C_4H_4O_4$) C, H, N.

3,4-Dihydro-*N*-[(2*S*)-3-[(2-methoxyphenyl)thio]-2-ethoxypropyl]-2*H*-(3*R*)-1,5-benzoxathiepin-3-amine (20). Compound **20** is purified by flash column chromatography (silica gel, dichloromethane). Crystallization of **20** as a maleate salt gave a white powder: mp = 142 °C; IR (KBr) ν 3450, 2969, 1693, 1577, 1476 cm^{-1}; ^1H NMR (DMSO-d_6) δ 1.11 (t, $J = 6.8$ Hz, 3H), 3.11−3.34 (m, 6H), 3.49 (m, 1H), 3.63 (m, 1H), 4.01 (s, 5H), 4.31 (d, $J = 13.2$ Hz, 1H), 4.46 (d, $J = 12.4$ Hz, 1H), 6.05 (s, 2H), 6.94−7.10 (m, 4H), 7.21−7.27 (m, 2H), 7.35 (d, $J = 7.4$ Hz, 1H), 7.41 (d, $J = 7.4$ Hz, 1H); ^{13}C NMR (DMSO-d_6) δ 15.1, 31.2, 32.2, 47.1, 55.6, 57.0, 64.2, 70.7, 73.9, 111.0, 120.9, 121.9, 123.4, 124.1, 126.3, 127.2, 128.6, 128.9, 131.5, 135.3 (2C), 156.6, 159.2, 167.0 (2C); $[\alpha]_D^{25}$ −9.5° (*c* 0.26, CH_3OH); HPLC Chiralpak AD-H (Daicel) eluting with heptane/isopropanol/diethylamine, 95:4.9:0.1 (1 mL/min, UV, 220 nm), $t_R = 12.7$ min, 93.6% dr; MS (ESI) $m/z = 406$ [MH^+]. Anal. ($C_{21}H_{27}NO_3S_2 \cdot C_4H_4O_4$) C, H, N.

3,4-Dihydro-*N*-[(2*S*)-3-[(2-methoxyphenyl)thio]-2-*n*-propoxypropyl]-2*H*-(3*R*)-1,5-benzoxathiepin-3-amine (21). Compound **21** is purified by flash column chromatography (silica gel, dichloromethane/ethyl acetate, 97:3). Crystallization of **21** as a maleate salt gave a white powder: mp = 158 °C; IR (KBr) ν 2959, 1618, 1575, 1470 cm^{-1}; ^1H NMR (DMSO-d_6) δ 0.85 (t, $J = 7.4$ Hz, 3H), 1.50 (m, 2H), 3.12−3.42 (m, 7H), 3.51 (m, 1H), 3.84 (m, 5H), 4.32 (d, $J = 13.2$ Hz, 1H), 4.48 (d, $J = 12.3$ Hz, 1H), 6.07 (s, 2H), 6.94−7.10 (m, 4H), 7.21−7.27 (m, 2H), 7.35 (d, $J = 7.5$ Hz, 1H), 7.41 (d, $J = 7.6$ Hz, 1H); ^{13}C NMR (DMSO-d_6) δ 10.8, 22.9, 31.6, 32.7, 47.4, 56.0, 57.4, 70.8, 71.1, 74.5, 111.4, 121.4, 122.4, 123.8, 124.6, 126.8, 127.7, 128.8, 129.1, 132.0, 135.8 (2C), 157.1, 159.7, 167.6 (2C); $[\alpha]_D^{25}$ −15° (*c* 0.30, CH_3OH); HPLC Chiralpak AD-H (Daicel) eluting with heptane/isopropanol/diethylamine, 95:4.9:0.1 (1 mL/min, UV, 220 nm), $t_R = 10.9$ min, 95.2% dr; MS (ESI) $m/z = 420$ [MH^+]. Anal. ($C_{22}H_{29}NO_3S_2 \cdot C_4H_4O_4$) C, H, N.

3,4-Dihydro-*N*-[(2*S*)-3-[(2-methoxyphenyl)thio]-2-ethylpropyl]-2*H*-(3*R*)-1,5-benzoxathiepin-3-amine (25). Crystallization of **25** as a fumarate salt gave a white powder: mp = 88 °C; IR (KBr) ν 2962, 1706, 1577, 1474 cm^{-1}; ^1H NMR (DMSO-d_6) δ 0.88 (t, $J = 7.0$ Hz, 3H), 1.47 (m, 2H), 1.72 (m, 1H), 2.76−2.82 (m, 2H), 2.85−3.05 (m, 3H), 3.14 (d, $J = 14.0$ Hz, 1H), 3.28 (s, 1H), 3.81 (s, 3H), 4.08 (dd, $J = 12.3$, 4.8 Hz, 1H), 4.22 (d, $J = 11.6$ Hz, 1H), 6.61 (s, 2H), 6.91−7.02 (m, 4H), 7.14−7.21 (m, 2H), 7.29 (d, $J = 7.3$ Hz, 1H), 7.35 (d, $J = 7.3$ Hz, 1H); ^{13}C NMR (DMSO-d_6) δ 10.6, 23.6, 32.8, 33.9, 38.6, 48.0, 55.5, 57.7, 73.5, 110.6, 120.9, 121.9, 123.6, 124.9, 126.3, 127.3, 127.4, 128.4, 131.5, 134.3 (2C), 156.2, 159.6, 166.5 (2C); $[\alpha]_D^{25}$ −8° (*c* 0.51, CH_3OH); HPLC Chiralcel OD (Daicel) eluting with hexane/isopropanol, 95:5 (1 mL/min, UV, 220 nm), $t_R = 16.6$ min, 96.6% dr; MS (ESI) $m/z = 390$ [MH^+]. Anal. ($C_{21}H_{27}NS_2O_2 \cdot C_4H_4O_4$) C, H, N.

3,4-Dihydro-*N*-[(2*S*)-3-[(2-methoxyphenyl)thio]-2-*n*-propylpropyl]-2*H*-(3*R*)-1,5-benzoxathiepin-3-amine (26). Crystallization of **26** as a maleate salt gave a white powder: mp = 132 °C; IR (KBr) ν 2950, 1623, 1577, 1470 cm^{-1}; ^1H NMR (DMSO-d_6) δ 0.87 (t, $J = 6.8$ Hz, 3H), 1.32 (m, 2H), 1.46 (dd, $J = 13.6$, 7.6 Hz, 2H), 2.08 (m, 1H), 2.97−3.19 (m, 4H), 3.30 (d, $J = 4.8$ Hz, 2H), 3.82 (s, 3H), 3.99 (s, 1H), 4.37 (d, $J = 13.2$ Hz, 1H), 4.47 (d, $J = 12$ Hz, 1H), 6.06 (s, 2H), 6.94−7.01 (m, 4H), 7.18−7.27 (m, 2H), 7.30 (d, $J = 7.6$ Hz, 1H), 7.40 (d, $J = 7.6$ Hz, 1H); ^{13}C NMR (DMSO-d_6) δ 13.9, 18.6, 31.0, 32.7, 32.8, 34.8, 48.3, 55.6, 57.8, 70.5, 110.8, 120.9, 122.0, 124.0, 126.2, 126.7, 127.8, 127.9, 128.7, 131.4, 135.5 (2C), 156.4, 159.0, 167.1 (2C); $[\alpha]_D^{25}$ −12.7° (*c* 0.43, CH_3OH); HPLC Chiralpak AD (Daicel) eluting with hexane/ethanol, 97:3 (1 mL/min, UV, 220 nm), $t_R = 8.6$ min, 94.3% dr; MS (ESI) $m/z = 404$ [MH^+]. Anal. ($C_{22}H_{29}NS_2O_2 \cdot C_4H_4O_4$) C, H, N.

3,4-Dihydro-*N*-[(2*S*)-3-[(2-methoxyphenyl)thio]-2-isopropylpropyl]-2*H*-(3*R*)-1,5-benzoxathiepin-3-amine (27). Crystallization of **27** as a maleate salt gave a white powder: mp = 115 °C; IR (KBr) ν 3429, 2975, 1575, 1474 cm^{-1}; ^1H NMR (DMSO-d_6) δ 0.89 (d, $J = 6.8$ Hz, 3H), 0.93 (d, $J = 6.8$ Hz, 3H), 1.90 (m, 1H), 2.02 (m, 1H), 2.93 (dd, $J = 12.4$, 6.2 Hz, 1H), 3.00−3.11 (m, 3H), 3.28−3.33 (m, 3H), 3.81 (s, 3H), 4.32 (d, $J = 12.8$ Hz, 1H), 4.44 (m, 1H), 6.04 (s, 2H), 6.94−7.00 (m, 2H), 7.04−7.10 (m, 2H), 7.18−7.25 (m, 2H), 7.31 (dd, $J = 7.6$, 1.1 Hz, 1H), 7.4 (d, $J = 7.6$ Hz, 1H); ^{13}C NMR (DMSO-d_6) δ; $[\alpha]_D^{25}$ −29.6° (*c* 0.36, CH_3OH);

HPLC Chiralpak AD (Daicel) eluting with hexane/ethanol, 97:3 (1 mL/min, UV, 220 nm), t_R = 8.6 min, 94.3% dr; MS (ESI) *m/z* = 404 [MH^+]. Anal. ($C_{22}H_{29}NS_2O_2 \cdot C_4H_4O_4$) C, H, N.

General Method for Ring-Opening of Epoxides 13 by 3-Amino-1,5-benzoxathiepine. To a solution of compound **13** (1 equiv) and 3-amino-1,5-benzoxathiepine (1 equiv) in 2-propanol (10 mL/mmol) was added sodium carbonate (5 equiv). The mixture was heated at reflux until completion of the reaction and then cooled to room temperature. The solvent was removed under reduced pressure and then the residue taken up in dichloromethane and washed with water and brine, dried over Na_2SO_4, filtered, and concentrated in vacuo. The free base was purified by flash column chromatography.

3,4-Dihydro-*N*-[3-[(2-methoxyphenyl)thio]-2-hydroxypropyl]-2*H*-(3*R*)-1,5-benzoxathiepin-3-amine (18ab). Crystallization of **18ab** as maleate salt gave a white powder: mp = 128 °C; IR (KBr) ν 3349, 3067, 1577, 1473 cm^{-1}; ^1H NMR (DMSO-d_6) δ 2.98−3.09 (m, 3H), 3.26 (d, J = 4.4 Hz, 2H), 3.33 (m, 1H), 3.83 (s, 3H), 3.87 (s, 1H), 3.99 (m, 1H), 4.26 (d, J = 13.2 Hz, 0.5H), 4.32 (d, J = 13.2 Hz, 0.5H), 4.44 (m, 1H), 5.85 (s, 1H), 6.03 (s, 3H), 6.95−7.02 (m, 2H), 7.06−7.11 (m, 2H), 7.19−7.26 (m, 2H), 7.32 (d, J = 7.6 Hz, 1H), 7.40−7.43 (m, 1H); $[\alpha]_D^{25}$ +29° (*c* 0.48, CH_3OH); HPLC Chiralcel OD (Daicel) eluting with hexane/ethanol, 80:20 (1 mL/min, UV, 220 nm), t_R = 15.6 min, 50.5% and t_R = 19.3 min, 49.2%; HPLC purity: 99.7% (Xbridge C8, 5 μM, acetonitrile−water−KH_2PO_4, 300:700:6.8 g, pH 4). Anal. ($C_{19}H_{23}NO_3S_2 \cdot C_4H_4O_4$) C, H, N.

3,4-Dihydro-*N*-[3-[(2-methoxyphenyl)thio]-2-hydroxypropyl]-2*H*-(3*S*)-1,5-benzoxathiepin-3-amine (18cd). Crystallization of **18cd** as a maleate salt gave a white powder: mp = 126 °C; IR (KBr) ν 3397, 3006, 1618, 1572 cm^{-1}; ^1H NMR (DMSO-d_6) δ 2.98−3.09 (m, 3H), 3.26 (d, J = 4.8 Hz, 2H), 3.27−3.39 (m, 2H), 3.83 (s, 3H), 3.87 (s, 1H), 3.99 (m, 1H), 4.26 (d, J = 12.4 Hz, 0.5H), 4.32 (d, J = 12.4 Hz, 0.5H), 4.46 (m, 1H), 5.85 (s, 1H), 6.03 (s, 3H), 6.97−7.02 (m, 2H), 7.06−7.11 (m, 2H), 7.19−7.26 (m, 2H), 7.32 (d, J = 7.5 Hz, 1H), 7.40−7.42 (m, 1H); $[\alpha]_D^{25}$ −26.2° (*c* 0.31, CH_3OH); HPLC Chiralcel OD (Daicel) eluting with heptane/ethanol, 80:20 (1 mL/min, UV, 220 nm), t_R 14.6 min, 48.8% and t_R 18.1 min, 48.7%; HPLC purity: 99.9% (Xbridge C8, 5μM, acetonitrile−water−KH_2PO_4, 300:700:6.8 g, pH 4). Anal. ($C_{19}H_{23}NO_3S_2 \cdot C_4H_4O_4$) C, H, N.

3,4-Dihydro-*N*-[(2*S*)-3-[(2-methoxyphenyl)thio]-2-hydroxypropyl]-2*H*-(3*R*)-1,5-benzoxathiepin-3-amine (18a). Crystallization of **18a** as a maleate salt gave a white powder: mp = 138 °C; IR (KBr) ν 3416, 2920, 1577, 1473 cm^{-1}; ^1H NMR (DMSO-d_6) δ 3.02−3.09 (m, 3H), 3.28 (m, 2H), 3.36 (d, J = 12.7 Hz, 1H), 3.83 (s, 3H), 3.90 (s, 1H), 4.01 (m, 1H), 4.34 (d, J = 12.6 Hz, 1H), 4.50 (dd, J = 13.6, 2.8 Hz, 1H), 5.09 (s, 1H), 6.06 (s, 2H), 6.97−7.10 (m, 4H), 7.19−7.25 (m, 2H), 7.32 (d, J = 7.4 Hz, 1H), 7.39 (d, J = 7.6 Hz, 1H); ^{13}C NMR (DMSO-d_6) δ 31.1, 35.4, 48.8, 55.6, 56.8, 65.5, 70.4, 110.9, 120.9, 121.0, 123.7, 124.2, 126.3, 126.8, 127.7, 128.9, 131.7, 137.7 (2C), 156.3, 159.2, 167.2 (2C); $[\alpha]_D^{25}$ −60.3° (*c* 0.74, CH_3OH); HPLC Chiralcel OD (Daicel) eluting with hexane/ethanol, 80:20 (1 mL/min, UV, 220 nm), t_R = 15.8 min, 97% dr; MS (ESI) *m/z* = 378 [MH^+]. Anal. ($C_{19}H_{23}NO_3S_2 \cdot C_4H_4O_4$) C, H, N.

3,4-Dihydro-*N*-[(2*R*)-3-[(2-methoxyphenyl)thio]-2-hydroxypropyl]-2*H*-(3*R*)-1,5-benzoxathiepin-3-amine (18b). Crystallization of **18b** as a maleate salt gave a white powder: mp = 136 °C; IR (KBr) ν 3503, 2925, 1625, 1572, 1458 cm^{-1}; ^1H NMR (DMSO-d_6) δ 2.99−3.09 (m, 3H), 3.27 (d, J = 4.9 Hz, 2H), 3.38 (d, J = 12.5 Hz, 1H), 3.83 (s, 3H), 3.83 (s, 1H), 4.02 (m, 1H), 4.28 (d, J = 13.2 Hz, 1H), 4.45 (dd, J = 13.6, 3.3 Hz, 1H), 5.90 (s, 1H), 6.06 (s, 2H), 6.97−7.11 (m, 4H), 7.21−7.22 (m, 2H), 7.33 (d, J = 7.6 Hz, 1H), 7.43 (d, J = 7.6 Hz, 1H); ^{13}C NMR (DMSO-d_6) δ 31.2, 35.3, 48.9, 55.6, 56.8, 65.4, 70.4; 110.9, 121.0, 122.0, 123.8, 124.3, 126.7, 126.8, 127.6, 129.0, 131.6, 135.6 (2C), 156.3, 159.4, 167.2 (2C); $[\alpha]_D^{25}$ −3.2° (*c* 0.43, CH_3OH); HPLC Chiralcel OD (Daicel) eluting with hexane/ethanol, 80:20 (1 mL/min, UV, 220 nm), t_R = 20.0 min, 94.5% dr; MS (ESI) *m/z* = 378 [MH^+]. Anal. ($C_{19}H_{23}NO_3S_2 \cdot C_4H_4O_4$) C, H, N.

3,4-Dihydro-*N*-[(2*S*)-3-[(2-methoxyphenyl)thio]-2-methylcarbonyloxypropyl]-2*H*-(3*R*)-1,5-benzoxathiepin-3-amine (22). A solution of 3,4-dihydro-*N*-[(2*S*)-3-[(2-methoxyphenyl)thio]-2-methylcarbonyloxypropyl]-2*H*-(3*R*)-1,5-benzoxathiepin-3-*tert*-butoxycarbonylamine (1.9 g, 3.65 mmol) in dichloromethane (10 mL) was treated with a 4 N aqueous solution of hydrogen chloride (20 mL). The reaction mixture was stirred overnight at room temperature and then slowly poured into a 1 N aqueous solution of sodium hydroxide and extracted with dichloromethane. The combined organic layer was washed with water and brine, dried over Na_2SO_4, filtered, and concentrated in vacuo. The compound of the title was purified by flash column chromatography (silica gel, cyclohexane/ethylacetate, 70:30). Crystallization of **22** as a maleate salt gave a white powder: mp = 130 °C; IR (KBr) ν 2955, 2834, 1745, 1578, 1473 cm^{-1}; ^1H NMR (DMSO-d_6) δ 1.95 (s, 3H), 3.15−3.31 (m, 5H), 3.39 (d, J = 12.1 Hz, 1H), 3.74 (s, 1H), 3.82 (s, 3H), 4.28 (d, J = 12.8 Hz, 1H), 4.37 (d, J = 12.6 Hz, 1H), 5.15 (m, 1H), 6.07 (s, 2H), 6.94−7.08 (m, 4H), 7.21−7.26 (m, 2H), 7.39 (d, J = 7.5 Hz, 2H); ^{13}C NMR (DMSO-d_6) δ 20.8, 31.7, 32.1, 46.8, 55.6, 57.4, 69.3, 71.0, 111.0, 120.9, 121.9, 122.9, 124.0, 126.5, 127.3, 128.7, 128.8, 131.5, 134.9 (2C), 156.7, 159.2, 167.0 (2C), 169.9; $[\alpha]_D^{25}$ +19.8° (*c* 0.26, CH_3OH); HPLC Chiralpak AD (Daicel) eluting with heptane/ethanol, 80:20 (1 mL/min, UV, 220 nm), t_R = 11.3 min, 99.4% dr; MS (ESI) *m/z* = 420 [MH^+]. Anal. ($C_{21}H_{25}NO_4S_2 \cdot C_4H_4O_4$) C, H, N.

3,4-Dihydro-*N*-[(2*S*)-3-[(2-methoxyphenyl)thio]-2-phenylcarbonyloxypropyl]-2*H*-(3*R*)-1,5-benzoxathiepin-3-amine (23). 3,4-Dihydro-*N*-[(2*S*)-3-[(2-methoxyphenyl)thio]-2-phenylcarbonyloxypropyl]-2*H*-(3*R*)-1,5-benzoxathiepin-3-*tert*-butoxycarbonylamine (1.47 g, 2.4 mmol) was treated as described for product **22**.The compound of the title was purified by flash column chromatography (silica gel, dichloromethane/ethylacetate, 93:7). Crystallization of **23** as a maleate salt gave a white powder: mp = 172 °C; IR (KBr) ν 3057, 2985, 2935, 1731, 1575, 1451 cm^{-1}; ^1H NMR (DMSO-d_6) δ 3.24 (m, 2H), 3.28−3.44 (m, 2H), 3.55 (m, 2H), 3.78 (s, 3H), 3.86 (s, 1H), 4.35 (d, J = 12.4 Hz, 1H), 4.44 (d, J = 12.3 Hz, 1H), 5.46 (m, 1H), 6.08 (s, 2H), 6.93−6.96 (m, 2H), 7.05−7.07 (m, 2H), 7.17−7.24 (m, 2H), 7.39 (d, J = 7.6 Hz, 1H), 7.44 (d, J = 7.3 Hz, 1H), 7.51 (t, J = 7.6 Hz, 2H), 7.67 (t, J = 7.5 Hz, 1H), 7.94 (d, J = 7.5 Hz, 2H); ^{13}C NMR (DMSO-d_6) δ 31.6, 32.5, 46.9, 55.6, 57.5, 70.0, 70.8, 111.0, 120.9, 121.8, 122.8, 124.0, 126.4, 127.4, 128.5, 128.7, 128.8, 129.4, 129.5, 131.5, 133.4, 134.7 (2C), 156.7, 159.1, 165.2, 167.1 (2C); $[\alpha]_D^{25}$ +55.1° (*c* 0.46, CH_3OH); HPLC Chiralpak AD (Daicel) eluting with heptane/ethanol, 80:20 (1 mL/min, UV, 220 nm), t_R = 11.4 min, 99.9% dr; MS (ESI) *m/z* = 482 [MH^+]. Anal. ($C_{26}H_{27}NO_4S_2 \cdot C_4H_4O_4$) C, H, N.

3,4-Dihydro-*N*-[3-[(2-methoxyphenyl)thio]-2-methylenepropyl]-2*H*-(3*R*)-1,5-benzoxathiepin-3-amine (24). A suspension of (*R*)-3-amino-1,5-benzoxathiepine (0.41 g, 2.26 mmol) and **15** (0.42 g, 1.81 mmol) and sodium carbonate (0.19 g, 1.81 mmol) in ethanol (5 mL) was heated at 100−110 °C for 24 h. The reaction mixture was cooled to room temperature, and then the solvent was evaporated off. The residue was taken up in dichloromethane and washed with water and brine, dried over Na_2SO_4, filtered, and concentrated in vacuo. The title compound was purified by flash column chromatography (silica gel, dichloromethane/methanol, 98:2). Crystallization of **24** as an oxalate salt gave a white powder: mp = 155 °C; IR (KBr) ν 3003, 2834, 1708, 1654, 1475 cm^{-1}; ^1H NMR (DMSO-d_6) δ 3.18−3.28 (m, 2H), 3.61 (m, 1H), 3.64−3.71 (m, 4H), 3.82 (s, 3H), 4.30 (dd, J = 12.8, 3.7 Hz, 1H), 4.37 (d, J = 11.2 Hz, 1H), 5.12 (s, 1H), 5.20 (s, 1H), 6.91 (t, J = 7.4 Hz, 1H), 6.97−7.06 (m, 3H), 7.19−7.24 (m, 2H), 7.28 (d, J = 6.8 Hz, 1H), 7.36 (d, J = 6.8 Hz, 1H); ^{13}C NMR (DMSO-d_6) δ 32.0, 34.9, 47.3, 55.6, 56.5, 71.5, 110.9, 118.3, 120.8, 121.8, 123.0, 123.9, 126.6, 127.3, 128.6, 129.3, 131.4, 138.1, 156.9, 159.2, 163.7 (2C); $[\alpha]_D^{25}$ +27.5° (*c* 0.43, CH_3OH); HPLC Chiralpak AD (Daicel) eluting with heptane/ethanol/diethylamine, 95:5:0.1 (1 mL/min, UV, 220 nm), t_R = 22.5 min, 95.2% dr; MS (ESI) *m/z* = 374 [MH^+]. Anal. ($C_{20}H_{23}NO_2S_2 \cdot C_2H_2O_4$) C, H, N.

3,4-Dihydro-*N*-[3-[(2-methoxyphenyl)thio]-2-(methyl-2-propene)-propyl]-2*H*-(3*R*)-1,5-benzoxathiepin-3-amine (28). Compound **28** was prepared in an analogous manner as that described for compound **24**. Purification by flash column chromatography (silica gel, dichloromethane/methanol, 97:3) and then crystallization of **28** as a maleate salt gave a white powder: mp = 155 °C; IR (KBr) ν 2900, 1575, 1474, 1359 cm^{-1}; ^1H NMR (DMSO-d_6) δ 1.65 (s, 3H), 1.86 (s, 3H), 2.51 (s, 2H), 3.32 (d, J = 5.2 Hz, 2H), 3.58−3.84 (m, 2H), 3.81 (s, 3H), 3.89 (s, 1H), 4.37 (d, J = 12.0 Hz, 1H), 4.49 (d, J = 11.2 Hz, 1H), 6.05 (s, 2H), 6.92−7.04 (m, 2H), 7.05−7.10 (m, 2H), 7.22−7.47 (m, 3H), 7.60 (d, J = 8.8 Hz, 1H); ^{13}C NMR (DMSO-d_6) δ 20.6, 21.0, 31.3, 32.6, 45.0, 55.6, 57.2, 70.6, 110.7, 119.6, 120.7, 121.9, 123.9, 124.1, 126.3, 127.5, 128.8, 130.0, 131.5, 135.6 (2C), 140.9, 157.1, 159.1, 167.1 (2C); $[\alpha]_D^{25}$ +24.1° (c 0.17, CH_3OH); HPLC Chiralpak AD (Daicel) eluting with heptane/ethanol/diethylamine, 95:5:0.1 (1 mL/min, UV, 220 nm), t_R = 22.5 min, 95.2% dr; MS (ESI) m/z = 402 [MH^+]. Anal. ($C_{22}H_{27}NO_2S_2 \cdot C_4H_4O_4$) C, H, N.

Conformational Analysis. Structures were built using version 7.3 of SYBYL molecular modeling software from Tripos Inc. running on Fuel Silicon Graphics workstation. Starting geometries were generated with the SKETCH builder from SYBYL. Geometry optimizations were carried out using the Tripos force field including the electrostatic term calculated from Gasteiger and Marsili atomic charges.

The folded conformation shown (see Figure 1) represents only a local minimum among 10 other within 10 kcal/mol of the global minimum.

Biology. Animals used in this study were housed and tested in an Association for the Assessment and Accreditation of Laboratory Animal Care (AAALAC) accredited facility in strict compliance with all applicable regulations, and the protocol was carried out in compliance with French regulations and local Ethical Committee guidelines for animal research. For in house use, KC 12291 was prepared according to the method reported in EP 5 547 967 (Kali-Chemie Pharma GmbH); Ivabradine was prepared according to FR 2 681 862 (Adir et Compagnie); Ranolazine was prepared according to EP 0 126 449 (Syntex Inc.). Veratridine was purchased from Sigma and TTX from Tocris Bioscience.

Ion Channel Pharmacology. The cell culture and patch clamp experiments were performed as described previously.[49] The internal solution (pipet) contained the following (in mmol): NaCl 10, CsCl 110, $CaCl_2$ 1, HEPES 10, EGTA 10, Mg-ATP 5, D-glucose 10, pH 7.3 (CsOH). The external solution contained the following for patch clamp experiments (in mmol): NaCl 30, CsCl 100, $MgCl_2$ 2, $CaCl_2$ 2, HEPES 10, D-glucose 5, pH 7.4 (CsOH). All experiments were carried out at room temperature (19−22 °C). Sodium current was elicited by depolarizing pulses (350 ms) from a holding potential value of −110 to −30 mV delivered at a frequency of 0.2 Hz. In order to verify the stability of voltage clamp, every five pulses, the holding potential was shifted to −90 mV for one pulse. Sodium current was elicited by square depolarizing pulses of 350 ms duration from a holding potential of −110 to −30 mV delivered at a frequency of 0.2 Hz. In order to verify the stability of voltage clamp, every five pulses, the holding potential was shifted to −90 mV for one pulse. Sodium current presenting an incomplete inactivation was induced with the alkaloid veratridine (40 μM). The late I_{Na} was measured as the mean current amplitude of the last 10 ms of the pulse (which is the magnitude of I_{Na} at 340−350 ms of the depolarizing pulse). Wild-type HEK 293 cells did not exhibit any peak and late inward sodium current (data not shown). The compound was dissolved in 50% DMSO in distilled water as 10 mmol of stock solution prepared freshly for each experiment. The final concentration of DMSO was 0.1%. All values are expressed as mean values ± SEM. Intragroup statistical analysis of results (P1, drug versus baseline) involves Tukey's test after testing for analysis of variance (ANOVA) with repeated measures. Intergroup statistical analysis of results (P2, drug versus vehicle) was performed using one-way analysis of variance followed by Dunnett's test if ANOVA was significant. Any P value lower than 0.05 was considered significant (StatView 4.1, Abacus Concepts, Berkeley, CA).

Veratridine-Induced Contracture in Rats Isolated Atria. Male Wistar rats (400−450 g, OFA, Iffa-Credo, France) were maintained at 20 ± 3 °C with constant humidity of 55 ± 5%, a 12 h light−dark cycle, and free access to food and tap water. The procedure is adapted from that described by Tamareille.[50] After a 30 min equilibration period, a single concentration of drug or vehicle was injected into the organ bath. Fifteen minutes later, veratridine (40 μM) was added. Systolic isometric tension development was measured before drug or solvent injection and just before the addition of veratridine in order to detect any positive or negative inotropic drug or vehicle effects. The maximum amplitude of veratridine induced contracture was measured irrespective of time.

Global Ischemia in Guinea Pig Isolated Hearts. Female guinea pigs (SPF, Hartley, Charles River, France), weighing 500−600 g, were used in the present study. The experiment was performed as described previously.[39] In brief, hearts excised from guinea pigs were placed in cold (4 °C) modified Krebs medium containing (in mmol) 124.6 NaCl, 4 KC1, 1.1 $MgSO_4$, 0.3 NaH_2PO_4, 1.8 $CaCl_2$, 24.9 $NaHCO_3$, and 11.1 D-glucose, pH 7.4, continuously with 95% O_2 + 5% CO_2 and mounted on a Langendorff system. A latex balloon was inserted through the left atrium and mitral valve into the left ventricle. Isovolumetric systolic and diastolic LVP, left ventricular developed pressure (LVDP = systolic-diastolic pressure), left ventricular end diastolic pressure, heart rate, positive $dP\,dt^{-1}{}_{max}$, negative $dP\,dt^{-1}{}_{max}$, and coronary flow were measured at 37 ± 1 °C with a constant perfusion pressure of 800 mmH_2O. The following parameters were measured: systolic and diastolic left ventricular pressure, left ventricular developed pressure, heart rate, positive dP/dt_{max}, negative dP/dt_{max}, and coronary flow. During perfusion under constant pressure, changes in coronary flow directly reflect changes in coronary vascular resistance. After 45−60 min of equilibration, the buffer solution containing vehicle or compound was perfused for 15 min. Global normothermic ischemia was then induced by clamping coronary flow for 50 min and was followed by 60 min of reperfusion. One drug concentration was evaluated per heart.

Regional Myocardial Ischemia in Anesthetized Rabbits. Animals (2.2−2.5 kg, New Zealand white, ESD France) were anesthetized by sodium pentobarbital (30−40 mg/kg, iv) via the ear vein. Anesthesia was maintained by intravenous injections of sodium pentobarbital as needed. The body temperature of animals was maintained at 38−39 °C with a heating pad throughout the experiment. Animals were connected to a respirator (683 rodent/small animal ventilator, Harvard Apparatus) for positive intermittent pressure and were ventilated with room air enriched with oxygen. A polyethylene fluid-filled catheter was introduced into the carotid artery for blood pressure measurements. Drug or vehicle was administered via the ear vein catheter. A four-limb ECG was recorded in lead II for determination of ST segment amplitude changes. The thorax was opened at the level of the fourth intercostal space, and a ligature was placed around the left coronary artery to induce regional myocardial ischemia. The ECG was examined for signs of myocardial damage (persistent increase in ST segment amplitude above 0.25 mV). If such signs occurred, the animal was excluded from the study. After the stabilization period, the first 5-min coronary artery occlusion was performed to verify the ST segment elevation (if ST segment elevation changes were less than 2-fold the baseline ST segment amplitude, the animal was excluded from the study). Then the occlusion was fully released for 30 min (reperfusion period). Five minutes before the end of reperfusion, the compound or its vehicle (a mixture of 40% polyethylene glycol 300 in sterile saline 0.9%) was administered over 1 min. A second coronary occlusion was performed. The ligature was tightened at the end of the experiment to estimate the proportion of the left ventricular mass subjected to ischemia. ST segment changes are expressed as the percentage (±SEM) of the mean maximal control ST segment increase.

Acknowledgment. The authors thank Y. Verscheure, J. L. Maurel, S. Brunel, and M. Borras, who contributed to this project. We thank Dr. J. P. Ribet and P. Zalavari for analytical support and Dr. P. Schambel for modeling studies. L. Petitpas' assistance for bibliographic searches is also very much appreciated.

Supporting Information Available: Experimental details and analytical data for intermediates **4**−**15**; methods for cells culture and isolation of cardiac myocytes. This material is available free of charge via the Internet at http://pubs.acs.org.

References

(1) (a) Catterall, W. A. Structure and function of voltage-sensitive ion channel. *Science* **1988**, *241*, 50–61. (b) Fozzard, H. A.; Hank, D. A. Structure and function of voltage-dependent sodium channels: comparison of brain II and cardiac isoforms. *Physiol. Rev.* **1996**, *76*, 887–926. (c) Carmeliet, E. Cardiac ionic currents and acute ischemia: from channels to arrhythmias. *Physiol. Rev.* **1999**, *79*, 917–1017. (d) Abriel, H. Roles and regulation of the cardiac sodium channel $Na_V1.5$: recent insights from experimental studies. *Cardiovasc. Res.* **2007**, *76*, 381–389.

(2) (a) Zilberter, Y. I.; Starmer, C. F.; Starobin, J.; Grant, A. O. Late Na channels in cardiac cells: the physiological role of background Na channels. *Biophys. J.* **1994**, *67*, 153–160. (b) Richmond, J. E.; Featherstone, D. E.; Hartmann, H. A.; Ruben, P. C. Slow inactivation in human cardiac sodium channels. *Biophys. J.* **1998**, *74*, 2945–2952.

(3) Saint, D. A. The cardiac persistent sodium current: an appealing therapeutic target. *Br. J. Pharmacol.* **2007**, *1*, 10.

(4) Maltsev, V. A.; Silverman, N.; Sabbah, H. N.; Undrovinas, A. I. Chronic heart failure slows late sodium current in human and canine ventricular myocytes: implications for repolarization variability. *Eur. J. Heart Failure* **2007**, *9*, 219–227.

(5) With elevated intracellular Na^+ levels at depolarized membrane potentials, the Na^+/Ca^{2+} exchanger (NCX) operates in reverse mode, importing Ca^{2+} instead of extruding it: Wei, G.-Z.; Zhou, J.-J.; Wang, B.; Wu, F.; Bi, H.; Wang, Y.-M.; Yi, D.-H.; Yu, S.-Q.; Pei, J.-M. Diastolic Ca(2+) overload caused by Na(+)/Ca(2+) exchanger during the first minutes of reperfusion results in continued myocardial stunning. *Eur. J. Pharmacol.* **2007**, *572*, 1–11. Increase of intacellular Ca^{2+} concentration may also cause spontaneous release of Ca^{2+} from the cytoplasmic reticulum.

(6) Leblanc, N.; Hume, J. R. Sodium current-induced release of calcium from sarcoplasmic reticulum. *Science* **1990**, *248*, 372–376.

(7) Hartmann, M.; Decking, U. K. M. R 56865 exerts cardioprotective properties independent of the intracellular Na^+-overload in the guinea pig heart. *Naunyn-Schmiedeberg's Arch. Pharmacol.* **2003**, *368*, 160–165.

(8) (a) Ver Donck, L.; Borgers, M.; Verdonck, F. Inhibition of sodium and calcium overload pathology in the myocardium: a new cytoprotective principle. *Cardiovasc. Res.* **1993**, *27*, 349–357. (b) Belardinelli, L.; Shryock, J. C.; Fraser, H. Inhibition of the late sodium current as a potential cardioprotective principle: effects of the late sodium current inhibitor ranolazine. *Heart* **2006**, *92* (Suppl. 4), 6–14.

(9) Narahashi, T. Pharmacology of tetrodotoxin. *J. Toxicol., Toxin Rev.* **2001**, *20*, 67–84.

(10) (a) Baer, M.; Best, P. M.; Reuter, H. Voltage-dependent action of tetrodotoxin in mammalian cardiac muscle. *Nature* **1976**, *263*, 344–345. (b) Coraboeuf, E.; Deroubaix, E.; Coulombe, A. Effect of tetrodotoxin on action potentials of the conducting system in the dog heart. *Am. J. Physiol.* **1979**, *236*, 561–567.

(11) Featherstone, D. E.; Richmond, J. E.; Ruben, P. C. Interaction between fast and slow inactivation in Skm1 sodium channels. *Biophys. J.* **1996**, *71*, 3098–3109.

(12) Valenzuela, C.; Bennett, P. B. Gating of cardiac Na^+ channels in excised membrane patches after modification by alpha-chymotrypsin. *Biophys. J.* **1994**, *67*, 161–171.

(13) Catterall, W. A.; Goldin, A. L.; Waxman, S. G., Jr. International Union of Pharmacology. XXXIX. Compendium of voltage-gated ion channels: sodium channels. *Pharmacol. Rev.* **2003**, *55*, 575–578.

(14) Vaughan Williams, E.M. Class I Drugs Inhibit the Fast Inward Sodium Current. Classification of Antiarrhythmic Action. In *Handbook of Experimental Pharmacology*; Vaughan Williams, E. M., Campbell, T. J., Eds.; Springer-Verlag: Berlin, Germany, 1989; Vol. 89, pp 45−67.

(15) (a) West, J. W.; Patton, D. E.; Scheuer, T.; Wang, Y.; Goldin, A. L.; Catterall, W. A. A cluster of hydrophobic amino acid residues required for fast Na(+)-channel inactivation. *Proc. Natl. Acad. Sci. U.S.A.* **1992**, *89*, 10910–10914. (b) McPhee, J. C.; Ragsdale, D. S.; Scheuer, T.; Catterall, W. A. A critical role for the transmembrane segment IVS6 of the sodium channel alpha subunit in fast inactivation. *J. Biol. Chem.* **1995**, *270*, 12025–12034. (c) Chahine, M.; Deschenes, I.; Trottier, E.; Chen, L.-Q.; Kallen, R. G. Restoration of fast inactivation in an inactivation-defective human heart sodium channel by the cysteine modifying reagent benzyl-MTS: analysis of IFM-ICM mutation. *Biochem. Biophys. Res. Commun.* **1997**, *233*, 606–610. (d) McPhee, J. C.; Ragsdale, D. S.; Scheuer, T.; Catterall, W. A. A critical role for the S4-S5 intracellular loop in domain IV of the sodium channel alpha-subunit in fast inactivation. *J. Biol. Chem.* **1998**, *273*, 1121–1129. (e) Rolh, C. A.; Boeckman, F. A.; Baker, C.; Scheuer, T.; Catterall, W. A.; Klevit, R. E. Solution structure of the sodium channel inactivation gate. *Biochemistry* **1999**, *38*, 855–861. (f) Maeda, Y.; Nakagawa, T.; Kuroda, Y. Helix-stabilizing effects of the pentapeptide KIFMK and its related peptides on the sodium channel inactivation gate peptides. *J. Pept. Res.* **2001**, *58*, 413–423.

(16) (a) Eaholtz, G.; Scheuer, T.; Catterall, W. A. Restoration of inactivation and block of open sodium channels by an inactivation gate peptide. *Neuron* **1994**, *12*, 1041–1048. (b) Ghatpande, A. S.; Sikdar, S. K. Competition for binding between veratridine and KIFMK: an open channel blocking peptide of the RIIA sodium channel. *J. Membr. Biol.* **1997**, *160*, 177–182. (c) Eaholtz, G.; Zagotta, W. N.; Catterall, W. A. Kinetic analysis of block of open sodium channels by a peptide containing the isoleucine, phenylalanine, and methionine (IFM) motif from the inactivation gate. *J. Gen. Physiol.* **1998**, *111*, 75–82. (d) Eaholtz, G.; Colvin, A.; Leonard, D.; Taylor, C.; Catterall, W. A. Block of brain sodium channels by peptide mimetics of the isoleucine, phenylalanine, and methionine (IFM) motif from the inactivation gate. *J. Gen. Physiol.* **1999**, *113*, 279–294. (e) Grant, A. O.; Chandra, R.; Keller, C.; Carboni, M.; Starmer, C. F. Block of wild-type and inactivation-deficient cardiac sodium channels IFM/QQQ stably expressed in mammalian cells. *Biophys. J.* **2000**, *79*, 3019–3035. (f) Wang, S.-Y.; Wang, G. K. Block of inactivation-deficient cardiac Na(+) channels by acetyl-KIFMK-amide. *Biochem. Biophys. Res. Commun.* **2005**, *329*, 780–788. (g) Bouhours, M.; Luce, S.; Sternberg, D.; Willer, J. C.; Fontaine, B.; Tabti, N. A1152D mutation of the Na^+ channel causes paramyotonia congenita and emphasizes the role of DIII/S4-S5 linker in fast inactivation. *J. Physiol.* **2005**, *565*, 415–427.

(17) This type of sulfur−aryl interaction is precedented in protein: Tatko, C. D.; Waters, M. L. Investigation of the nature of the methionine−π interaction in β-hairpin peptide model systems. *Protein Sci.* **2004**, *13*, 2515–2522. However, we could not confirm the existence of such an interaction in solution (NOESY experiments performed on the commercially available Ac-KIFMK-NH_2 peptide [156162-44-6]).

(18) This working hypothesis would imply that such a folded conformation has physiologic relevance. By no means we contend (1) that such a folded conformation exists under physiological conditions, especially when the IFM is buried within the channel protein, (2) that it represents a bioactive conformation, and (3) that compounds of this work mimic such conformation. The merit of the modeling was to direct attention toward heterocycles containing an aryl−thioether linkage.

(19) Ranolazine: *N*-(2,6-dimethylphenyl)-4-[2-hydroxy-3-(2-methoxyphenoxy)propyl]-1-piperazineacetamide [95635-55-5]. This compound is claimed to be a late sodium currents blocker: Schram, G.; Zhang, L.; Derakhchan, K.; Ehrlich, J. R.; Belardinelli, L.; Nattel, S. Ranolazine: ion-channel-blocking actions and in vivo electrophysiological effects. *Br. J. Pharmacol.* **2004**, *142*, 1300–1308.

(20) (a) Vacher, B.; Castan-Cuisiat, F.; John, G.; Le Grand, B. Benzoxathiepin Derivatives and Their Use as Medicines. WO 02/081464, 2002 (Pierre Fabre Médicament). (b) Compound **2a** is currently undergoing phase I clinical studies. For further information, see the following: Pignier, C.; Letienne, R.; Vacher, B.; Delhon, A.; Le Grand, B. Antiischemic activities of F 15845, a new blocker of the persistent cardiac sodium current. *Acta Pharmacol. Sinica* **2006**, *27* (1), 169. Pignier, C.; Letienne, R.; Vacher, B.; Delhon, A.; Le Grand, B. F 15845: a voltage-dependent persistent sodium current blocker. *Eur. Heart J.* **2006**, *27*, S1.

(21) KC 12291, 3,4-dimethoxy-*N*-methyl-[3-[(5-phenyl-1,2,4-thiadiazol-3-yl)oxy]propyl]benzeneethanamine [181935-23-9]. See the following: John, G. W.; Létienne, R.; Le Grand, B.; Vacher, B.; Patoiseau, J.-F.; Colpaert, F. C.; Coulombe, A. KC 12291: an atypical sodium channel blocker with myocardial anti-ischemic properties. *Cardiovasc. Drug Rev.* **2004**, *22*, 17–26.

(22) Ivabradine, 7,8-dimethoxy-3-(3-(((1*S*)(4,5-dimethoxybenzocyclobutan-1-yl)methyl)methylamino)propyl)-1,3,4,5-tetrahydro-2*H*-benzazepin-2-one [155974-00-8]. DiFrancesco, D.; Camm, J. A. Heart rate lowering by specific and selective If current inhibition with ivabradine. A new therapeutic perspective in cardiovascular disease. *Drugs* **2004**, *64*, 1757–1765. Ruzyllo, W.; Tendera, M.; Ford, I.; Fox, K. M. Antianginal efficacy and safety of ivabradine compared with amlodipine in patients with stable effort angina pectoris. *Drugs* **2007**, *67*, 393–405.

(23) (*S*)-3-(1-Oxopentyl)-4-(phenylmethyl)-2-oxazolidinone [143868-89-7]. Lister, T.; Perkins, M. V. Total synthesis of a hemiacetal polypropionate from *Siphonaria australis*. *Aust. J. Chem.* **2004**, *57*, 787–797.

(24) Evans, D. A.; Urpi, F.; Somers, T. C.; Clark, J. S.; Bilodeau, M. T. New procedure for the direct generation of titanium enolates. Diastereoselective bond construction with representative electrophiles. *J. Am. Chem. Soc.* **1990**, *112*, 8215–8216.

(25) Ihara, M.; Katsumata, A.; Setsu, F.; Tokunaga, Y.; Fukumoto, K. Synthesis of six-membered compounds by environmentally friendly cyclization using indirect electrolysis. *J. Org. Chem.* **1996**, *61*, 677–684.

(26) Soucy, F.; Grenier, L.; Behnke, M. L.; Destree, A. T.; McCormack, T. A.; Adams, J.; Plamondon, L. A novel and efficient synthesis of a highly active analogue of *clasto*-lactacystin β-lactone. *J. Am. Chem. Soc.* **1999**, *121*, 9967–9976.

(27) Ihara, M.; Setsu, F.; Shohda, M.; Taniguchi, N.; Tokunaga, Y.; Fukumoto, K. Asymmetric total synthesis of tacamonine (pseudovincamone I) via radical cyclization. *J. Org. Chem.* **1994**, *59*, 5317–5323.

(28) (*S*)-**8a2**: 2-ethyl-1,3-propanediol mono(4-methylbenzenesulfonate) [470453-95-3]. (*S*)-**8a4**: 2-(1-methylethyl)-1,3-propanediol mono(4-methylbenzenesulfonate) [470454-42-3]. See ref 20a. See also the following: Schmid, R.; Wirz, B. Preparation of Optically Active Propanediol Monoesters as Intermediates for Pharmaceuticals. WO 880883 (Hoffmann-La Roche).

(29) See Supporting Information for **9a5**: (*S*)-3-[(2-methoxyphenyl)thio]-2-fluoro-propan-1-ol.

(30) **6a6**: 3-[(2-methoxyphenyl)thio]propanal, R_1 = H [124829-86-3]. Hiratsuka, M.; Shiroshita, M.; Ohtsuka, S.; Arai, K.; Hirata, N. Preparation and Dehydration of 4-Hydroxy-6-phenylthio-2-hexanones as Herbicide Intermediates. EP 323915 (Sumitomo Chemical Co., Ltd.).

(31) Evans, D. A.; Ng, H. P.; Rieger, D. Total synthesis of the macrolide antibiotic rutamycin B. *J. Am. Chem. Soc.* **1993**, *115*, 11446–11459.

(32) Vacher, B.; Brunel, Y.; Castan-Cuisiat, F. An Improved Process for the Preparation of Benzoxathiepines and Their Intermediates. WO 2005/103027, 2005 (Pierre Fabre Medicament).

(33) (*S*)-**10**: 1-(3-hydroxy-2-hydroxypropylthio)-2-methoxybenzene [470453-82-8]. See ref 20a.

(34) Kim, M.-J.; Choi, Y. K. Lipase-catalyzed enantioselective transesterification of *O*-trityl 1,2-diols. Practical synthesis of (*R*)-triglycidol. *J. Org. Chem.* **1992**, *57*, 1605–1607.

(35) (a) 3-Chloro-2-(chloromethyl)propene [1871-57-4]. Lynch, K. M.; Dailey, W. P. 3-Chloro-2-(chloromethyl)propene. *Org. Synth.* **1998**, *75*, 89–97. (b) 1-Chloro-2-(chloromethyl)-3-methyl-2-butene [185320-38-1]. Werner, M.; Stephenson, D. S.; Szeimies, G. Synthesis of [1.1.1]propellanes by bridging of bicyclo[1.1.0]butanes. *Liebigs Ann. Chem.* **1996**, 1705–1715.

(36) (a) Lazdunski, M.; Renaud, J. F. The action of cardiotoxins on cardiac plasma membranes. *Annu. Rev. Physiol.* **1982**, *44*, 463–473. (b) Tikhonov, D. B.; Zhorov, B. S. Sodium channel activators: model of binding inside the pore and a possible mechanism of action. *FEBS Lett.* **2005**, *579*, 4207–4212.

(37) Wermelskirchen, D.; Wilffert, B.; Peters, T. Veratridine-induced intoxication: an in vitro model for the characterization of anti-ischemic compounds. *J. Basic Clin. Physiol. Pharmacol.* **1992**, *3*, 293–321.

(38) Le Grand, B.; Marty, A.; Vieu, S.; Talmant, J. M.; John, G. W. Veratridine-induced tetanic contracture of the rat isolated left atrium. Evidence for novel direct protective effects of prazosin and WB4101. *Naunyn-Schmiedeberg's Arch. Pharmacol.* **1993**, *348*, 184–190.

(39) Le Grand, B.; Vie, B.; Talmant, J. M.; Coraboeuf, E.; John, G. W. Alleviation of contractile dysfunction in ischemic hearts by slowly inactivating Na^+ current blockers. *Am. J. Physiol.* **1995**, *269*, H533–H540.

(40) This was verified on several compounds in this series (e.g., **17**, **19**). There was no isomerization of the compound under the conditions of in vitro and in vivo experiments.

(41) For instance, the compound bearing a gem-dimethyl group at C2 was totally inactive (data not shown).

(42) About bioisosteric equivalence of OH, OCH_3, and fluorine, see the following: Biffinger, J. C.; Kim, H. W.; DiMagno, S. G. The polar hydrophobicity of fluorinated compounds. *ChemBioChem* **2004**, *5*, 622–627. Paulini, R.; Mueller, K.; Diederich, F. Orthogonal multipolar interactions in structural chemistry and biology. *Angew. Chem., Int. Ed.* **2005**, *44*, 1788–1805.

(43) Late I_{Na} inhibition values may be underestimated in our in vitro system for several reasons: (1) the biophysical characteristics of the channels when expressed in nonexcitable cells (HEK-293) may change; (2) the pore-forming α-subunit ($Na_V1.5$) is expressed in the absence of auxiliary β-subunits; (3) I_{Na} was measured with veratridine present in the experiment, which may somehow affect the result. Also, patch clamp experiments were performed at 19−22 °C and not at physiological temperature.

(44) The selectivity of **2a** was assessed in regard to the main cardiac ionic currents. The compound did not significantly affect rapid I_{Na}, rat ventricular myocytes I_{to}, guinea pig ventricular myocytes inward rectifier I_{K1} and I_{Kr}, I_{Ks}, human $I_{K\text{-}erg}$ (HEK-293 cells), guinea pig ventricular myocytes I_{CaL}, I_{CaT}. No significant interaction of **2a** was detected against an extensive panel of GPCRs, uptake sites, enzymes, transporters, and exchangers.

(45) Verscheure, Y.; Pouget, G.; De Courtois, F.; Le Grand, B.; John, G. W. Attenuation by R 56865, a novel cytoprotective drug, of regional myocardial ischemia- and reperfusion-induced electrocardiographic disturbances in anesthetized rabbits. *J. Cardiovasc. Pharmacol.* **1995**, *25*, 126–133.

(46) In the same rabbit model the ED_{50} value after oral administration of **2a** is 0.13 mg/kg. The ratio ED_{50} po/iv = 2.6 suggests that **2a** is orally bioavailable in this species. In addition, the antiischemic profile observed in the rabbit model after iv administration is maintained but shifted po.

(47) In the anesthetized rabbit model of regional myocardial ischemia, we observed no significant variation in mean arterial pressure (MAP) but important variation of the cardiac frequency with ivabradine (bpm ± SEM): 0.04 mg/kg (−3.4 ± 1.9), 0.16 mg/kg (−20.7 ± 5.2), 0.63 mg/kg (−69.4 ± 8.8), 2.5 mg/kg (−112.6 ± 9.7). In comparison, there were no variations in MAP and heart rate with **2a** (bpm ± SEM): 0.01 mg/kg (−3.2 ± 1.4), 0.04 mg/kg (0.3 ± 2.1), 0.16 mg/kg (−6.4 ± 5.0), 0.63 mg/kg (−3.2 ± 2.9), 2.5 mg/kg (−8.6 ± 4.9).

(48) (a) Thom, T.; Haase, N.; Rosamond, W.; Howard, V. J.; Rumsfeld, J.; Manolio, T.; Zheng, Z.-J.; Flegal, K.; O'Donnell, C.; Kittner, S.; Lloyd-Jones, D.; Goff, D. C., Jr.; Hong, Y. Heart disease and stroke statistics. 2006 Update: a report from the American Heart Association Statistics Committee and Stroke Statistics Subcommittee. *Circulation* **2006**, *113*, e85–e151. (b) Abbate, A.; Biondi-Zoccai, G. G. L.; Agostoni, P.; Lipinski, M. J.; Vetrovec, G. W. Recurrent angina after coronary revascularization: a clinical challenge. *Eur. Heart J.* **2007**, *28*, 1057–1065. (c) Bankston, J. R.; Robert, S. K. Fading sodium channels in failing hearts. *Circ. Res.* **2007**, *101*, 1073–1074. (d) Albert, C. M.; Nam, E. G.; Rimm, E. B.; Jin, H. W.; Hajjar, R. J.; Hunter, D. J.; MacRae, C. A.; Ellinor, P. T. Cardiac sodium channel gene variants and sudden cardiac death in women. *Circulation* **2008**, *117*, 16–23. (e) George, C. H.; Barberini-Jammaers, S. R.; Muller, C. T. Refocussing therapeutic strategies for cardiac arrhythmias: defining viable molecular targets to restore cardiac ion flux. *Expert Opin. Ther. Pat.* **2008**, *18*, 1–19.

(49) Pignier, C.; Revenaz, C.; Rauly-Lestienne, I.; Cussac, D.; Delhon, A.; Gardette, J.; Le Grand, B. Direct protective effects of poly-unsaturated fatty acids, DHA and EPA, against activation of cardiac late sodium current: a mechanism for ischemia selectivity. *Basic Res. Cardiol.* **2007**, *102*, 553–564.

(50) Tamareille, S.; Le Grand, B.; John, G. W.; Feuvray, D.; Coulombe, A. Anti-ischemic compound KC 12291 prevents diastolic contracture in isolated atria by blockade of voltage-gated sodium channels. *J. Cardiovasc. Pharmacol.* **2002**, *40*, 346–355.

JM800100Z